الجمهورية الجزائرية الديمقراطية الشعبية
People's Democratic Republic of Algeria
وزارة التعليم العالي والبحث العلمي
Ministry of Higher Education and Scientific Research
جامعة غرداية
University of Ghardaia

Registration number
/…../…../…../…../…..

كلية العلوم والتكنولوجيا
Faculty of Science and Technology
قسم الآلية والكهروميكانيك
Department of Automatics and Electromechanics

End of study thesis, in view of obtaining the diploma

Master

Field: Automatic and Electromechanical
Sector: Automatique
Speciality: Automatic and system

Theme

Robust control by Takagi-Sugeno fuzzy models for a variable speed wind turbine based on a DFIG generator.

Presented by :
BENZAIT Abderrahmane
TFYECHE Mohammed

Sustained publicly on 11/06/2022

In front of the jury consisting by :

TIDJANI Naoual	**MCB**	**BDKM**	**Supervisor**
KIFFOUCHE Abdesslam	**MCB**	**Ghardaia**	**Co-Supervisor**
SKANDER Bouraghda	**MAA**	**Ghardaia**	**Examiner**
MOUSSA Oussama	**MAB**	**Ghardaia**	**Examiner**

College year 2021/2022

Dedications

“

First of all, we thank Almighty God for having given us Courage, willpower, patience, and health during all these university years and that it is thanks to him that this work can be carried out.

We would like to express our deep gratitude to our supervisor, Dr.Nawel Tidjani for her continuous monitoring and valuable advice.

Deep gratitude to all the teachers and other professors who allowed us to get here.

Gratitude to our family and to everyone dear to us and to all of you

Thank you

”

- B.Abderrahamane

- T.Mohammed

Abstract

Over the past ten years, electricity generation from wind turbines has increased eight times. This energy production is booming, and today there are various means The desires of researchers to finally explore it thoroughly. (DFIG) is a kind of Wind turbines have been the subject of many studies in recent years. It is Wind turbines work with the speed of the wind. Its main advantage is to be It consists of an asynchronous machine, a wound rotor and a power supply Supply of electric current through the stator and the rotor. This structure allows good performance Over a wide range of wind speeds at a reasonable cost. managed to be profitable Because it uses smaller sized transducers. Despite its advantages, there is a problem: Constantly changing wind force, resulting in permanent maximum power output. The goal of this research is to find a strategy for wind turbines to produce maximum power in all climates and under all wind conditions using T-S fuzzy control technology.

Keywords :

Doubly fed induction generator (DFIG),
Wind turbine,
direct current, (DC),
Asynchronous machine,
Takagi-Sugeno (T-S)

ملخص

على مدى السنوات العشر الماضية ، زاد توليد الكهرباء من توربينات الرياح ثماني مرات من ماكانت عليه. في هذا االسياق، الهياكل المرتبطة بتطوير مولدات توربينات الرياح تعد حاليا ذات أهمية كبرى في جميع المنشآت الصناعية.

عملنا هدا يركز بالاخص على المولد الحث ذو التغذية المزدوجة هو نوع من توربينات الرياح وقد كان موضوع العديد من الدراسات في السنوات الأخيرة. ومن توربينات الرياح المكونة من مغناطيسي دائم متزامن الذي يتم تحريكه بسرعة متغيرة وإمداد طاقة للتيار الكهربائي الغير المستمر عبر الجزء الثابت والدوار، يسمح هذا الهيكل بأداء جيد على نطاق واسع من سرعات الرياح بتكلفة معقولة. أن تكون مربحة لأنها تستخدم محولات طاقة أصغر حجمًا. وعلى الرغم من كثرة مزاياها ، إلا أنها تواجه بعض المشاكل: التغيير المستمر في قوة الرياح ، مما يؤدي إلى عدم إنتاج طاقة قصوى دائمة. الهدف من هذا البحث هو إيجاد وتطبيق التحكم من نوع الضبابي Takagi-Sugeno لتوربينات الرياح لإ نتاج أقصى في اى سرعت رياح متوفرة

كلمات مفتاحية :

توربينات الرياح

التيار الكهربائي الغير المستمر

آلة غير متزامنة

محولات طاقة

التحكم الغامض Takagi-Sugeno

RÉSUMÉ

Au cours des dix dernières années, la production d'électricité à partir d'éoliennes a augmenté huit fois. Cette production d'énergie est en plein essor, et il existe aujourd'hui différents moyens Les envies des chercheurs de l'explorer enfin de fond en comble. (DFIG) est une sorte de Les éoliennes ont fait l'objet de nombreuses études ces dernières années. Il est Les éoliennes fonctionnent avec la vitesse du vent. Son principal avantage est d'être Il se compose d'une machine asynchrone, d'un rotor bobiné et d'une alimentation Alimentation en courant électrique à travers le stator et le rotor. Cette structure permet de bonnes performances Sur une large gamme de vitesses de vent à un coût raisonnable. réussi à être rentable Parce qu'il utilise des transducteurs de plus petite taille. Malgré ses avantages, il y a un problème : Force du vent en constante évolution, résultant en une puissance de sortie maximale permanente. L'objectif de cette recherche est de trouver une stratégie pour que les éoliennes produisent une puissance maximale dans tous les climats et dans toutes les conditions de vent en utilisant la technologie de contrôle flou de Takagi Sugeno.

Mots clés :

Générateur à induction à double alimentation (DFIG),

Éolienne,

courant continu, (DC),

Machine asynchrone,

Takagi-Sugeno (T-S)

Acronyms

PMSM	*Permanent Magnet Synchronous machines*
VAWT	*Vertcall Axe Wind Turbine*
HAWT	*Horizontal Axe Wind Turbine*
MPPT	*Maximum Power Point Tracking*
DFIG	*Double-Fed Induction Generator*
DC	*Direct Current*
AC	*Alternative Current*
T–S	*Takagi Sugeno*
Cp	*Power Coefficient*
PI	*Proportional Integral*
WT	*Wind Turbine*
LMIs	*Linear Matrix Inqualities*
PDC	*Parallel Distributed Compensation*

Symbols

ρ	air density
λ	speed ratio
P_{aer}	aerodynamic power [W].
C_p	power coefficient
ρ	density of the air $(1.22kg/m3)$.
V	wind speed [m/s].
R	radius of the turbine in meters [m].
β	angle of the blade orientation [degree (°)]
C_{aer}	aerodynamic torque of the turbine [Nm].
C_g	the torque resulting from the multiplier.
G	multiplier ratio.
Ω_{mec}	generator speed [rad/s].
$\Omega_{turbine}$	turbine speed [rad/s].
J	the total inertia that appears on the generator rotor.
$J_{turbine}$	turbine inertia [kg.m2].
J_m	generator inertia[kg.m2].
C_{mec}	mechanical torque.
C_{em}	electromagnetic torque [Nm].
C_g	the torque resulting from the multiplier.
f	viscous coefficient of friction.
K	Static gain.
T	Time constant.
ω_n	natural pulsation.
ξ	damping coefficient.
p	number of pole pairs of the asynchronous machine.
σ	leakage coefficient.
ω_s	The rotational speed of the electromagnetic field of the stator.

Contents

List of Figures

Introduction

Today, an observation of an increase in the global average temperature faces a great concern caused by human activity [1]. The production of electrical energy relies almost entirely on the combustion of fossil fuels. Its ecological effect has led to the emergence of an increase in various types of pollution, thus modifying the energy balance and the temperature of the earth due to the increase in the concentrations of greenhouse gases. This causes the phenomenon of global warming on an unprecedented scale. Since the industrial revolution and technological advancements, the consumption of electrical energy has become more and more common and indispensable nowadays. This high consumption will lead to the depletion of fossil energy reserves. This is why, in the face of these impacts, a large-scale energy transition towards the development of new renewable energy sources is essential, in effect promoting their implementation as an alternative to fossil fuels. These energies are rather clean and can make up for the lack of energy production and meet this ever-increasing demand.

Renewable energies come from natural phenomena, such as the sun, wind, geothermal energy, and biomass. Their main characteristic is that they produce no polluting emissions during the operating phase. Today, the development of wind energy has evolved to become more efficient, with sustained momentum [2]. To improve behavior and optimize the production system, make it competitive at a lower cost and better control the quality of the service through clean and efficient energy. Wind energy consists of exploiting the kinetic energy of the wind transformed using an aero generator device. Appropriate control strategies allow the extraction of power, depending on meteorological conditions [3], thus ensuring a high rate of return.

The various control techniques require control and monitoring of the energy produced during the conversion chain before being injected into the network [4]. Linear controllers limit the ability to achieve control performance. Non-linear controllers are better suited to the conversion of the wind energy system, such as nonlinear adaptive control [5], neural network control [6], as well as sliding mode control [7]. In the presence of parametric variations, robust fuzzy controls of the Takagi-Sugeno type are better adapted in the presence of these disturbances, to better study the stability and system performance [8], [9]. The research work that we present in this document concerns the exploration production chain of wind energy. They fall within the framework of improvement in the performance of uncertain systems, which are subject to variations in internal parameters of the generator, to get the most out of it. The study conducted in our research aims to achieve these goals.

Chapter 1

GENERAL ON THE WIND TURBINE SYSTEM

1.1 Introduction

The principle of operation of wind turbines is mainly based on the aerodynamic conversion of the kinetic energy of the wind into mechanical energy. Then the generator, in turn, converts the mechanical energy of the wind into electrical energy. These different elements are designed to produce maximum power.

In this chapter, we give an overview of the different renewable energies, including wind energy. And discover the different types of wind turbines, then identify the main families of current wind turbines, namely fixed speed and variable speed wind turbines.

1.2 General context

The ever-increasing demands on energy, increasingly scarce fossil fuel resources, concerns about pollution, and the search for clean energy are the main drivers of renewable power generation. Renewable energy sources such as solar, wind, and tidal energy are clean, inexhaustible, and environmentally friendly energy sources. Due to all these factors, wind power has attracted a lot of attention in recent years. According to a global wind report 2022 , Fig 1.1 . The global wind industry had its second-best year in 2021, with almost 94 GW of capacity added globally, trailing behind the 2020's record growth by only 1.8%. However, this growth needs to quadruple by the end of the decade if the world is to stay on course for a 1.5C pathway and net-zero by 2050 by dispensing with unclean energy [10].

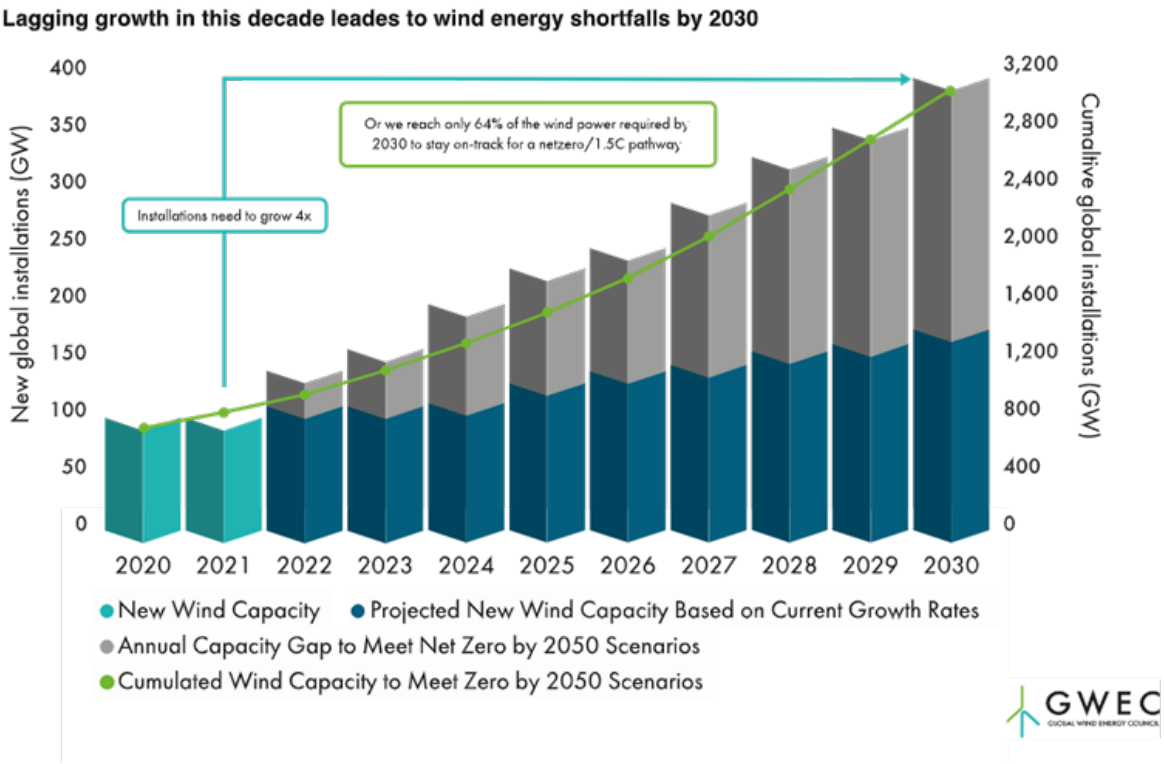

Figure 1.1: Global Wind Report 2022 [10].

The proliferation of wind turbines has led electrical engineering researchers to carry out investigations to improve the efficiency of electromechanical conversion and the quality of the energy supplied.

Joint progress in power electronics and digital electronics now makes it possible to address variable speed control in low, medium, and high power applications. Together with these technological advances, the scientific community has developed various control approaches to control the flux and torque of electrical machines in real-time, with the following advantages: high efficiency, low weight, small dimensions, fast operations, and very high power density.

The robust control of nonlinear systems is a current subject of study and the methods developed in the literature are numerous. We can cite by way of example and in a non-exhaustive way, the control methods type H-infinity, predictive, adaptive, neural, fuzzy, with variable structures, etc.

On the other hand, several types of electric machines have been used for energy conversion, however, it would seem that the asynchronous machine is essential in applications using wind turbines. Fixed-speed asynchronous machines must operate close to the synchronism speed because the network imposes the frequency. The rotor speed is almost constant. The advantage of variable speed for a wind system is to be able to operate over a wide range of wind speeds and to be able to extract the maximum power from it by the MPPT (Maximum Power Point Tracking) strategy, for each speed, for this type of application the double-fed asynchronous machine associated with power electronics converters is the most widely used machine today.

In this general context, our study focuses on the conversion of wind energy into electrical energy, which has become competitive thanks to three essential factors: the motivating nature of this energy, the development

of the wind turbine industry, the evolution of semiconductor technology, as well as new methods of controlling variable speed turbines. Nevertheless, several problems persist, linked on the one hand to the complexity of wind power conversion systems; namely, the necessity of the speed multiplier between the turbine and the generator, and the instability of the wind speed on the other hand.

1.3 History of wind energy

The use of wind energy has a long history, until the early 20th-century wind power was used to provide mechanical power to pump water or to grind grain. At the beginning of modern industrialization, the use of the fluctuating wind energy resource was substituted by fossil fuel-fired engines or the electrical grid, which provided a more consistent power source, and In the early 1970s, with the first oil price shock, the interest in the power of the wind re-emerged. This time, however, the main focus was on wind power providing electrical energy instead of mechanical energy. This way, it became possible to provide a reliable and consistent power source by using other energy technologies, via the electrical grid, as a backup.

In 1891, the Dane Poul LaCour was the first to build a wind turbine generating electricity. Danish engineers improved the technology during World War I and II and used the technology to overcome energy shortages. The wind turbines built by the Danish company F.L. Smidth in 1942 can be considered a forerunner of modern wind turbine generators [11].

During 1930s, the windmill popularity rose and reached its highest peak by the end of this period with more than 600,000 wind turbine units installed in farms and rural areas in the United States. Most of those wind machines were only able to produce less than 1 kW of electricity. The wind market started to slow down by the end of 1950 with the development in power lines construction technology, but before that, most of the farms were using wind generated electricity by means of the latest available technology of horizontal axis wind turbine, which was built in 1941 [12].

1.4 Types of renewable energy sources

Exploited for a long time – since antiquity for some of them (wind power, the power of rivers) – renewable energies became, in 1973, a topical subject during the first “oil shock”, within a framework of seeking energy security and independence. Then, with the awareness of the limited aspect of oil reserves, (the peak of production had already reached in many deposits, and oil resources could exhausted from the middle of the 19th century) and the need to fight against greenhouse gas emissions and air pollution, their development has become a major issue.

1.4.1 Solar Energy

Solar energy is the radiation emitted in all directions by the Sun. The Earth receives it at the rate of the average power of 1.4 kW/m2, for a surface perpendicular to the Earth-Sun direction. This solar flux is attenuated when crossing the atmosphere by absorption or diffusion, depending on the meteorological conditions and the latitude of the place, at ground level, the remaining power is of the order of one kW/m2. The amount of usable energy varies between 800 and 2,500 kWh/m2/year.

✣ The Solar Oven

The principle implemented is the concentration of the radiation, but with a multiplier factor much greater than in the previous case. The best example is the Odeillo solar oven, created in 1968 in Cerdagne (between Spain and France) In Odeillo, solar radiation is captured by a "field" of 63 adjustable flat mirrors of 45 m2 each, then reflected on a parabolic mirror made up of 9,500 elementary mirrors with sides of 0.45 m curved by mechanical stress. The convergent beam thus obtained makes it possible to reach a power of 1 MW, 1,000 times the power received on the ground; materials exposed to this radiation can be heated to temperatures of 1,500 to 3,800°C. Research focuses on reactions at high temperatures, the mechanical and electrical properties of materials, and the preparation of high purity refractory oxides.

✣ Photovoltaic

It is the direct transformation of solar radiation into electricity in a solar cell. The photovoltaic effect, i.e. the ability of semiconductor material to generate an electric current when struck by photons, was discovered in 1839 by Antoine Becquerel. It is usually produced in discs of monocrystalline silicon (made from crystallized silicon in a single crystal), polycrystalline (silicon in the form of a single crystal), or less frequently (their yield is still low or they are in the phase of development), in thin-layer materials: amorphous silicon (with a non-crystallized structure), cadmium tellurium, organic materials, etc. Multiple applications have been developed, from sensors and panels installed on homes to solar power stations (parabolic collectors or fields of solar panels), including calculators, watches, and streetlights. Car prototypes that can partly recharge their batteries using solar collectors are also studied.

1.4.2 Biomass Energy

Biomass is all the living beings present at a given time in an environment: trees, plants, algae, fungi, animals, and bacteria. They contain energy, derived directly or indirectly from solar energy; moreover, they constituted for millennia the only source of energy used by man: the food of man himself and of livestock, which was the only motors, and wood, the only fuel known until the discovery of fossil fuels.

- Thermochemical conversion: combustion, photosynthesis, gasification.
- Biochemical conversion: ethyl, methyl fermentation, anaerobic fermentation of plant waste.

1.4.3 Hydraulic Energy

Hydraulic wheels have long animated cereal mills, but also artisanal or industrial installations. The invention of the hydraulic turbine then the dynamo and finally the alternator opened an important way toward hydroelectricity which constitutes the source of renewable energy the most used in the world. The principle consists of creating a water reservoir by blocking the course of a river and using the potential energy of the accumulated water.

Depending on the height of fall, we distinguish between high-head plants, medium-head plants, and run-of-river plants. Different types of turbines are suitable for optimal operation depending on the type of fall. The production of electricity from the hydraulic origin is very flexible; it participates in the basic production of the networks, but can also come in addition to peak hours thanks to its speed of implementation. If its production price is low, the particularly high cost of investments must take into account. Hydroelectric dams also contribute to flood reduction.

1.4.4 Geothermal Energy

The Earth's core contains radioactive elements such as uranium, the decay of which produces heat (radioactivity). Apart from the sometimes-violent natural manifestations of volcanoes, this heat propagates towards the surface and heats aquifers located between 500 and 2,000 m deep. It is the deepest aquifers that brought to the highest temperature; the geothermal gradient, which is of the order of 3°C per 100 m, can reach 100°C per 100 m in the boundary zones of plates (tectonics).

Since the temperature of the subsoil is constant at a given depth, geothermal energy has the advantage of being independent of the climate and has a little negative impact on the environment.

Depending on the depth of the aquifers and the temperature of the water available, we distinguish between very low, low, medium, and high-energy geothermal energy.

1.4.5 Recovery Energy

Part of the waste from human activities can be transformed to use the energy it contains. Combustible waste (paper and cardboard, wood, and certain plastics) is incinerated; the heat produced is used to heat rooms.

The recovery of certain objects or materials, if it not directly producing energy, can help save energy. For example, the glass bottles collected thanks to the selective sorting set up in most localities make it possible to save raw material (mainly sand and limestone). In addition, the energy needed to produce the glass because the cullet resulting from glass recycling melts at 1000°C instead of 1500°C for mixing raw materials. In addition, the environment benefits from it.

1.4.6 Other New Energy Sources

- **Energy from the sea**

It can take various forms; that of the tides is of both solar and lunar origin; that of the waves results from the action of the wind, and finally, the temperature gradient between the surface waters and those of the funds is a source of thermal energy. Other avenues explored, such as osmotic plants, operating on the difference in salinity between fresh water and saltwater.

✣ **Tidal energy**

The difference in level between low tide and high tide must be sufficient for it to be exploitable. In France, the Rance tidal power plant commissioned in 1967 consists of a dam 750 m long and 27 m high closing the Rance estuary. At a rising tide as well as a falling tide, the water passes through each group and produces electricity; for one year, the average production is around 550 GWh. However, tidal power plants have the defect of profoundly modifying the ecosystems of estuaries.

1.4.7 Wind Energy

Wind power has been driving mills for even longer than waterpower; it was also the power source for ships. This form of energy is currently exploited by wind turbines and is used either directly to drive pumps, or indirectly by producing electric current (wind generators).

A wind turbine consists of a kind of propeller with a horizontal shaft, orientable with respect to the direction of the wind along a vertical axis. Many wind turbines of extremely simple construction are installed all over the world, and many operate a water pumping system necessary for domestic or agricultural use; a reserve of water can moreover be easily constituted to regularize its availability.

Modern horizontal-axis wind turbines are equipped with propellers whose blades have a profile similar to that of an airplane wing; the natural wind and due to the rotation of the blades give rise to a resultant force, one of the components which cause the rotation of the propeller while the other applied to the pylon. Vertical axis aero generators have made, their generally ovoid rotating ”wings” also have the profile of an airplane wing, and their operation is indifferent to the direction of the wind; they have the disadvantage of being expensive, and their yield is rather mediocre.

The power of wind turbines is proportional to the diameter of their rotor (alternator). The largest has a rotor 120 m in diameter (on a mast 120 m high), for a power of 6 million watts (MW).and there are wind turbines at sea, anchored offshore a few dozen meters deep. Floating wind turbines that can be installed far from the coast have also been developed. and wind generators can also couple with panels of solar cells and an accumulator battery to optimize the supply of electricity.

1.5 Development of wind energy in Algeria

Algeria has huge renewable energy potential, especially in the southern regions. The spatial distribution of the theoretical potential of wind energy is calculated, as shown in Fig 1.2. The results showed that the highest annual cumulative wind energy in the Ain Salah area (east of Adrar) was 3.33 MWh/m2/year. In addition, another important wind potential is observed in the highlands and north-western region of Algeria (Oran province). On the other hand, the area with the lowest potential is the area from the capital Algiers to the province of Bejaia (36.5°N, 4.4°E), with a total annual energy of about 380.84 kWh/m2/year. In general, the average wind power potential in Algeria is estimated at 1.90 MWh/m2/year [13].

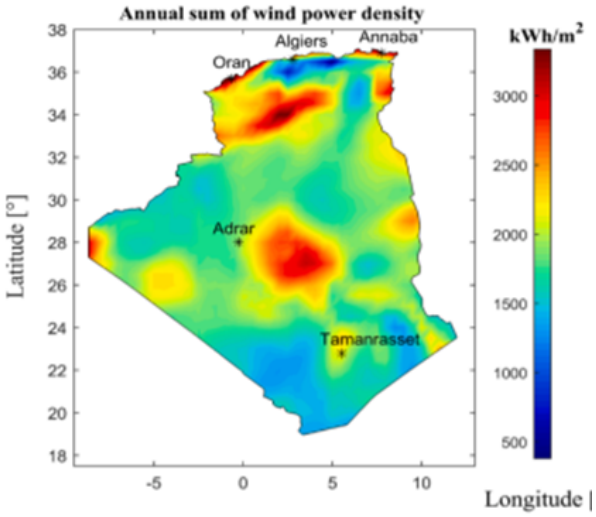

Figure 1.2: The sum of annual solar and the wind energy potential in Algeria over the year 2019.

Algeria is initiating a green energy dynamic by launching an ambitious program for the development of renewable energies (EnR) and energy efficiency. This vision of the Algerian government is based on a strategy focused on the development of inexhaustible resources such as solar energy and their use to diversify energy sources and prepare the Algeria of tomorrow. Thanks to the combination of initiatives and intelligence, Algeria is embarking on a new sustainable energy era Fig 1.3 .

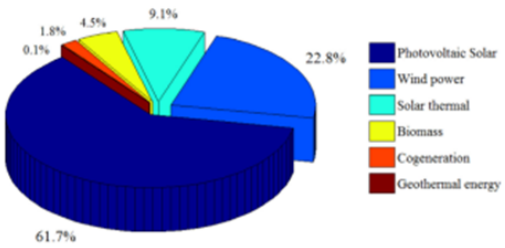

Figure 1.3: Distribution of development program of renewable energy technology sector [14].

The updated renewable energy program consists of installing power from renewable sources in the order of 22,000 MW by 2030 for the national market, with the maintenance of the export option as a strategic objective, if the market conditions permit Fig 1.4 [15].

The first wind farm project was located in Adrar in the Kabertene area with a power of 10 MW which represented 5% approximately of the electrical energy supplied by the local network.

Phases of the Algerian renewable energy program

Energy type	1st phase 2015–2020 [MW]	2nd phase 2021–2030 [MW]	Total [MW]
Photovoltaic	3000	10,575	13,575
Wind	1010	4000	5010
CSP	–	2000	2000
Cogeneration	150	250	400
Biomass	360	640	1000
Geothermal	05	10	15
Total	4525	17,475	22,000

Figure 1.4: Consistency of the renewable energy program.

1.6 Advantages and Drawbacks of Wind Energy

1.6.1 Advantages of Wind energy

- Wind energy is clean, reliable, economical, and ecological.
- Wind energy is a renewable, free, and inexhaustible energy.
- Wind energy is also not risky energy like nuclear energy and does not produce toxic or radioactive waste
- Among all the sources of electricity production, the wind source is by far subject to the strongest growth
- In addition to these many advantages, Wind Energy has other advantages, namely that it is flexible and can be perfectly adapted to the available capital as well as to Energy needs. In addition, the period of high productivity, often located in winter where the winds are strongest, corresponds to the period of the year when the energy demand is greatest. Another very important advantage of this type of Energy is the fact that it is not subject to variations in fuel costs (especially with the evolution of the price of a barrel of oil).

1.6.2 Drawbacks of wind energy

- The major drawback of this energy lies in the fact that the wind, the source of energy electricity produced, is a stochastic quantity; it varies over time and space. This variability is amplified by the fact that the energy is proportional to the cube of the wind speed. In the case of stand-alone installations, it is, therefore, necessary to use storage or to double the installation with a diesel generator, which increases the cost. In the case of grid coupling, wind turbines can lead to disruption of their stability. This problem becomes less and less important thanks to using power electronics. The most important effect of the wind turbine on the environment is its visual effect, so it is important to integrate it well into the landscape. The noise produced by a wind turbine is increasingly minimal, compared to that from a stream 50 to 100 meters away and certainly very low compared to traffic noise on-road or air [16].

1.7 Different types of wind turbine

Wind power systems can be classified according to their design, construction, type, or location such as.A distinction is made between wind turbines:

- ⋆ With a horizontal or vertical axis.
- ⋆ With a multiplier or direct drive.
- ⋆ Facing the wind or against the wind.
- ⋆ With one, two, three, or more blades.
- ⋆ Employing a pitch control or an aerodynamic stall for the system mechanical. for installation on land or at sea (Onshore or Offshore).

1.7.1 vertical axis wind turbines (VAWT)

They are called vertical axis wind turbines because the axis of rotation of the rotor is vertical and perpendicular to the direction of the wind. They are the first structures developed to produce electricity. the main vertical axis sensors are the Savonius rotor, the classical Darrieus rotor, and the H-shaped Darrieus Fig 1.5. this type of wind turbine can use two principles: differential drag or cyclic variation of incidence.

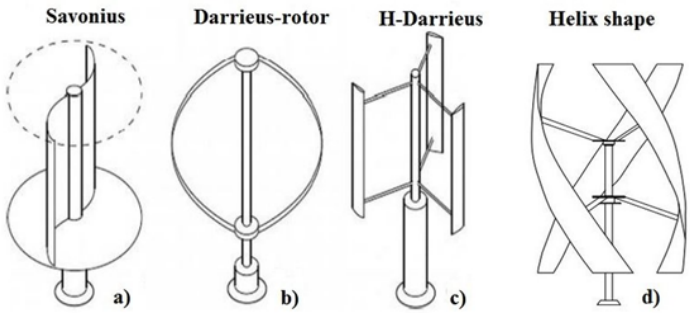

Figure 1.5: Various types of vertical wind turbines.

1.7.2 horizontal axis wind turbines (HAWT)

They are called horizontal axis wind turbines because the axis of rotation of the rotor is horizontal, parallel to the wind direction. They are simple in design, and usually feature two- or three-bladed propellers, or multi-bladed propellers for pumping water. There are two families of horizontal axis wind turbines: slow-running wind turbines and fast-running wind turbines Fig 1.6.

Figure 1.6: horizontal axis wind turbine.

According to its number of blades, the horizontal axis wind turbine is called a single blade, two blades, three blades, or multi-blades.A turbine with a horizontal axis of rotation remains facing the wind, like the propellers of airplanes and windmills. It is attached to the top of a tower, which allows it to capture a greater amount of wind energy. Most wind turbines installed are horizontal.

1.8 Betz's law

Let us consider the horizontal axis wind system represented in Fig 1.7 on which the wind speed V_1 upstream of the wind generator and the speed V_2 downstream have been represented. Assuming that the speed of the wind crossing the rotor is equal to the average between the speed of the undisturbed wind in front of the wind turbine V_1 and the speed of the wind after passing through the rotor V_2 , $\frac{V_1+V_2}{2}$ the moving air mass of density (ρ) crossing the surface (S) blades in one second is:

$$m = \frac{\rho \cdot S \cdot (V_1 + V_2)}{2} \tag{1.1}$$

The power P_m then extracted is expressed by half the product of the mass and the decrease in wind speed (Newton's second law):

$$P_m = \frac{m \cdot (V_1^2 - V_2^2)}{2} \tag{1.2}$$

Either by replacing m by its expression in (1.1):

$$P_m = \frac{\rho \cdot S \cdot (V_1 + V_2) \cdot (V_1^2 - V_2^2)}{2} \tag{1.3}$$

A theoretically undisturbed wind would cross this same surface (S) without a decrease in speed, i.e. at speed V_1 , the power P_{mt} corresponding would then be:

$$P_{mt} = \frac{1}{2} \cdot \rho \cdot S \cdot V_1^3 \tag{1.4}$$

The ratio between the power extracted from the wind and the total power theoretically available is then :

$$\frac{P_m}{P_{mt}} = \frac{(1 + \frac{V_1}{V_2}) \cdot (1 - (\frac{V_1}{V_2})^2)}{2} \tag{1.5}$$

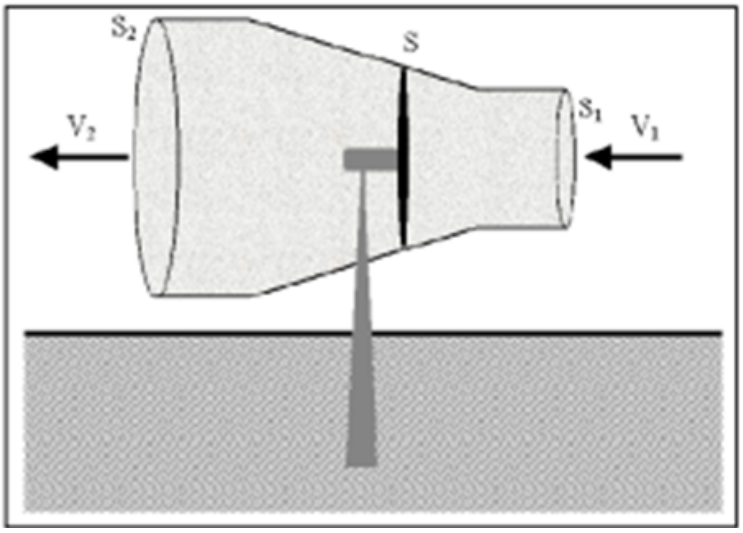

Figure 1.7: Current tube around a wind turbine.

If we represent the characteristic corresponding to the equation above (Fig 1.8), we see that the ratio $\frac{P_m}{P_{mt}}$ also called power coefficient "Cp" has a maximum of 16/27 or 0.59 . It is this theoretical limit called the Betz limit which fixes the maximum extractable power for a given wind speed. This limit is actually never reached and each wind turbine is defined by its own power coefficient expressed as a function of the relative speed "λ" representing the ratio between the speed of the end of the blades of the wind turbine and the speed of the wind Fig 1.9 [17].

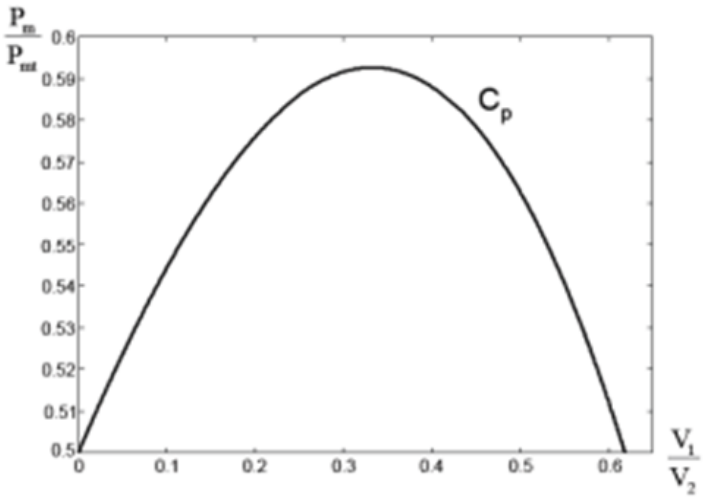

Figure 1.8: Power coefficient.

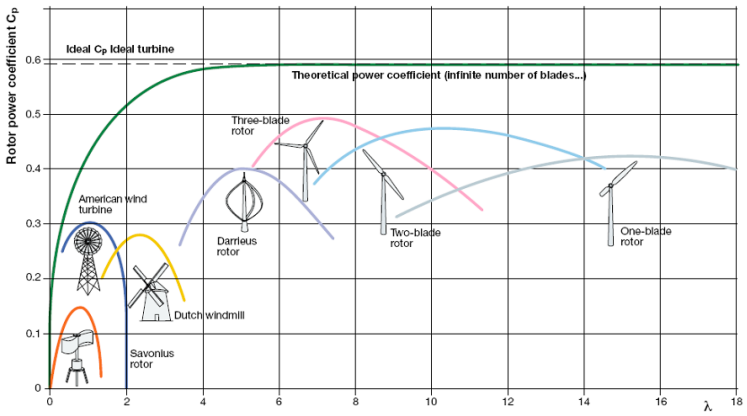

Figure 1.9: Power coefficient for different types of wind turbines.

1.9 Description of wind turbines

Wind turbines are made up of many parts. They are all A prerequisite for the correct operation of wind turbines. Fig 1.10 shows Different types of parts on wind turbines.

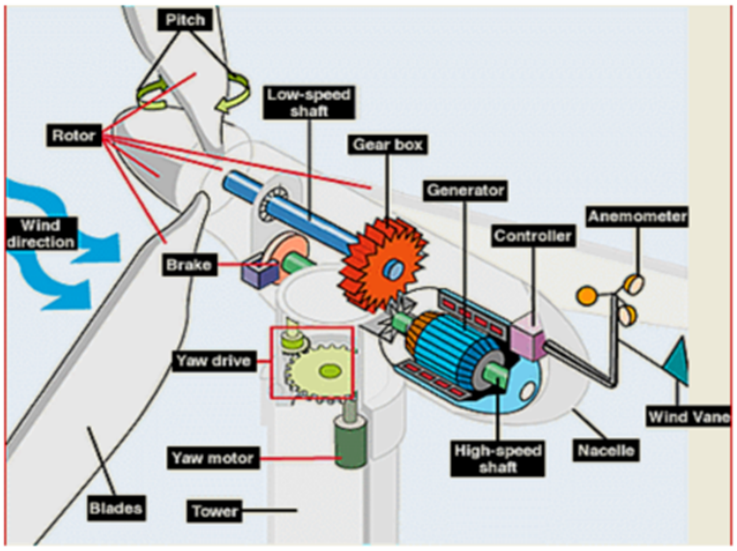

Figure 1.10: Wind turbine parts.

✣ The rotor

The main task of the rotor blades is to ”catch” the wind. This causes the blades to start spinning, producing rotational wave energy. It essentially converts kinetic energy into mechanical energy. This mechanical energy is then converted into electrical energy by various other components in the wind turbine. Furthermore, the power provided by the wind turbine can be correlated with the size of the wind turbine. The size of the rotor plays an important role in the amount of energy that can be harvested from the wind.

✣ Shaft

The wind-turbine shaft is connected to the center of the rotor. The shaft spins when the rotor spins. The

rotor transfers its rotational mechanical energy into the shaft which is connected to an electric generator on the other end.

✣ **Electric Generator**

Generators use the properties of electromagnetic induction to generate voltage. Central to the operation of all AC motors is the concept of a rotating field created by a set of static coils. There is also a set of windings in the rotor. Each rotation of the rotor shaft causes electromagnetic induction. A voltage is induced in the rotor conductors. A current is then generated in the coil, which directs the current through the distribution wire.Both induction generators and synchronous generators are commonly used in commercial wind turbines, but there are others.

✣ **Anemometer**

An anemometer is a device used to measure wind speed. The simplest anemometer is the cup anemometer. It has three hemispherical shells, each mounted on one of four horizontal arms. Each cup is mounted at an equal angle to the others. The airflow passes through the cup in each horizontal direction, causing the cup to rotate at a speed proportional to the wind speed.There is a factor called the anemometer factor, which determines the relationship between rotational speed and wind speed based on the size of the shell and arm.

1.10 Fixed Speed Wind Turbines and Variable Speed Wind Turbines

The two families of wind turbines connected to electrical networks can be classified according to their speed: namely fixed speed turbines and variable speed turbines.

1.10.1 Fixed speed

A fixed-speed wind turbine refers to the fact that its rotor always has the same operating angular speed regardless of wind speed. This speed of operation depends on the design of the turbine itself and the frequency of the network electric.

Since the beginning of the 1970s, with the arrival of the asynchronous machine in the field of wind power, almost all fixed-speed wind turbines use the cage asynchronous machine [18]. For this configuration, the machine stator asynchronous is connected directly to the network via a transformer Fig (1.12). Of moreover, this configuration couples the rotor of the wind turbine to the rotor of the asynchronous machine through a gearbox. The latter, paired with a number of pairs of poles of the electric generator, makes it possible to determine a fixed speed of operation. This configuration is used mainly at Vestas Wind Systems, Siemens and Nordex [18]. For

its part, the synchronous machine has many disadvantages for a such configuration. It is used only occasionally [19] and, for this reason, it will not be discussed in this document.

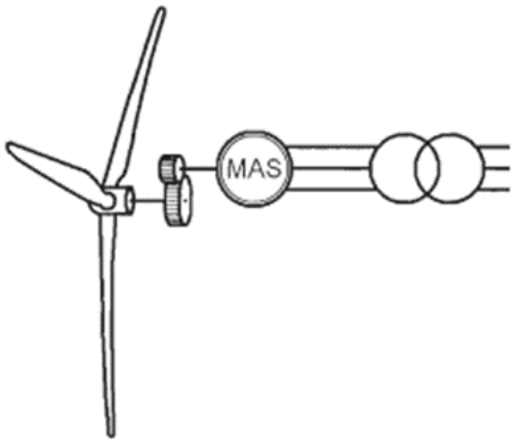

Figure 1.11: Fixed speed wind turbine using a squirrel-cage induction generator.

Since the wind turbine is at a fixed speed, regardless of the speed of the wind, the efficiency of the turbine, represented by the power coefficient C_p is optimal only for a single wind speed. Due to the variability of the wind speed, this wind turbine configuration allows fluctuations in the power produced and this can create instabilities on the network [20]. Fixed-speed wind turbines still have some advantages, namely the simplicity, the use of inexpensive technology and the low need for maintenance.

1.10.2 variable speed

Variable speed wind turbines are currently the most widely used in industry. The term variable speed refers to the fact that the speed of the turbine is independent of the power grid frequency. The main advantage of operating the turbine at variable speed is to maximize the capture of energy available in the wind. According to reference [21], a variable-speed wind turbine can extract 8 to 15% more energy from the wind annually than a fixed-speed wind turbine.

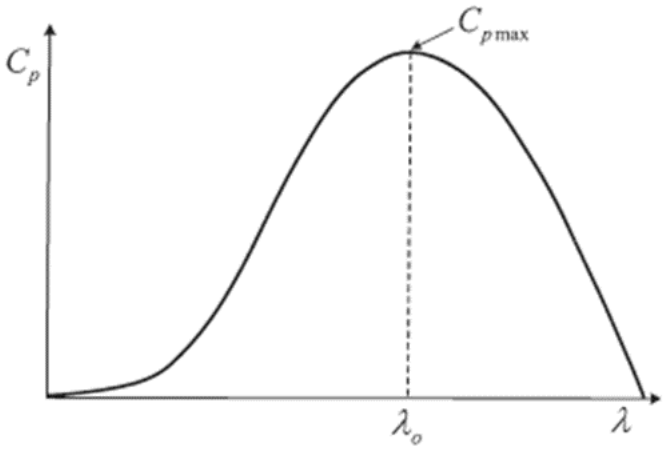

Figure 1.12: Fixed speed wind turbine using a squirrel-cage induction generator.

Fig 1.12 shows that for any pitch angle, the aerodynamic efficiency varies depending on the specific speed. The maximum power coefficient (C_{Pmax}) is reached when the specific speed is optimal (λ_0). As for her, the speed specific depends on the wind speed and the operating speed of the turbine. Therefore, it is possible to represent the mechanical power produced from the turbine as a function of rotor operating speed for different wind speeds, and this, always with a fixed pitch angle (Fig 1.13).

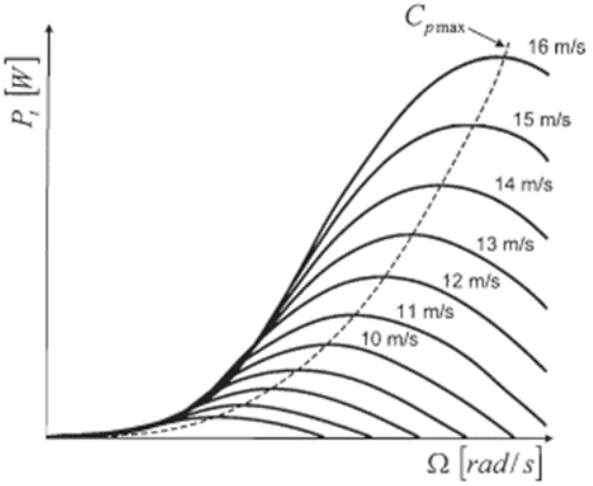

Figure 1.13: Turbine power as a function of rotor speed for different wind speeds.

Fig 1.13 presents an example of curves of the power produced as a function of rotor speed. On this one, we see that for each wind speed, the power has a maximum as a function of the rotor speed. Following these maximums, we can plot a curve on which the power coefficient is maximum. The place where the power coefficient is maximum also corresponds to the speed optimal specific. By modifying the operating speed of the turbine, it is possible to maintain a maximum power coefficient by playing on the specific speed and thus maintain turbine operation on the dotted curve. Therefore, to optimize the mechanical power produced from the energy contained in the wind, we must adjust the angular speed of the rotor as a function of wind speed. Only one configuration variable speed can manage to do this kind of optimization.

1.11 Conclusion

In this chapter, we have provided an overview of different renewable energies, including wind energy, based on the definition, its development history, and future prospects in Algeria. Then, the different types of generators and the nature of the electrical part are presented. In the next chapter, we will study the work of wind-chain conversion, which is based on a double-fed asynchronous machine.

Chapter 2

MODELING OF DFIG INTEGRATED INTO A WIND SYSTEM

2.1 Introduction

Currently, the majority of wind projects above 1 MW are based on the use of the rotor-driven asynchronous machine. The stator circuit is directly connected to the electrical network. The second circuit placed on the rotor is also connected to the network but via transducers.

This chapter mainly concerns the modeling and control of wind turbines. First the different types of machines, then the MPPT operating principle, and the Techniques for extracting the maximum power.

2.2 Various types of machines

Electric generators used in the field of wind energy are from Various types of synchronous machines, asynchronous machines, and asynchronous machines with Squirrel Cage machines and direct current machines. These are used to convert energy Rotation mechanism into electrical energy and can be directly connected to network or via a power adapter.

2.2.1 Synchronous

There are two types of synchronous machines present in wind energy, namely conventional synchronous machines and permanent magnet synchronous machines (PMSM). Conventional synchronous machines have an independent inductor circuit to produce a magnetic field that biases the rotor. This inductor circuit is made up of the machine's wound rotor, slip rings and brushes, and a DC source. In motor operation, the speed of rotation of the machine is imposed by that of the rotating magnetic field of the stator. The rotor is therefore driven at a so-called synchronous speed. As a generator, the variation of the magnetic field created by the rotor (or inductor) and seen by the stator windings induces an alternating voltage to the stator whose frequency corresponds to

the speed of rotation of the rotor. As regards machines with permanent magnets, the magnetic field polarizing the rotor is created by the presence of permanent magnets and makes it possible to eliminate the field circuit of the synchronous generator. The latter has high efficiency and power factor [22].

2.2.2 Asynchronous

Asynchronous machines are widely used as motors in industry, which makes a machine available in many models and has an advantageous cost. These machines represent a technology of choice for wind generators since they are of robust and inexpensive construction, they require little maintenance and they synchronize easily when they are connected directly to the network. In addition, the slip at the rotor makes it possible to absorb sudden changes in torque following significant wind turbulence. It is for these reasons that they represent 85% of the wind energy market. There are two types of asynchronous machines commonly used in wind energy, namely squirrel-cage asynchronous machines and double-fed asynchronous machines [22].

squirrel-cage asynchronous

Cage asynchronous machines are also called induction machines. The squirrel cage refers to the shape that the rotor has. This name comes from the fact that these machines do not have an inductor circuit, as in the case of the synchronous machine; we therefore only have access to the stator. Their principle of operation is as follows: as a motor, the stator produces a magnetic field rotating at synchronous speed using a three-phase AC power supply and a configuration of its windings in different poles. The rotating magnetic field in turn induces voltage and current in the rotor windings. The torque is created by the interaction between the rotating stator magnetic field and the rotor magnetic field itself created by the currents flowing in the rotor windings. To maintain a current in the rotor windings, the rotor must rotate at a speed slower than the synchronous speed.

double-fed asynchronous

Doubly-fed electric machines are basically electric machines that are fed ac currents into both the stator and the rotor windings. Most doubly-fed electric machines in the industry today are three-phase wound-rotor induction machines [23].

The principle of the DFIG is that stator windings are connected to the grid and rotor winding are connected to the converter via slip rings and a back-to-back voltage source converter that controls both the rotor and the grid currents. Thus rotor frequency can freely differ from the grid frequency (50 or 60 Hz).

The primary advantage of doubly-fed induction generators when used in wind turbines is that they allow the amplitude and frequency of their output voltages to be maintained at a constant value, no matter the speed of the wind blowing on the wind turbine rotor. Other advantages include the ability to control the power factor while keeping the power electronics devices in the wind turbine at a moderate size.

The back-to-back converter consists of two converters, i.e., machine-side converter and grid-side converter

that are connected back-toback. Between the two converters a dc-link capacitor is placed, as energy storage, in order to keep the voltage variations (or ripple) in the dc-link. A more detailed picture of the DFIG system with a back-to-back converter can be seen in Fig 2.1 [23].

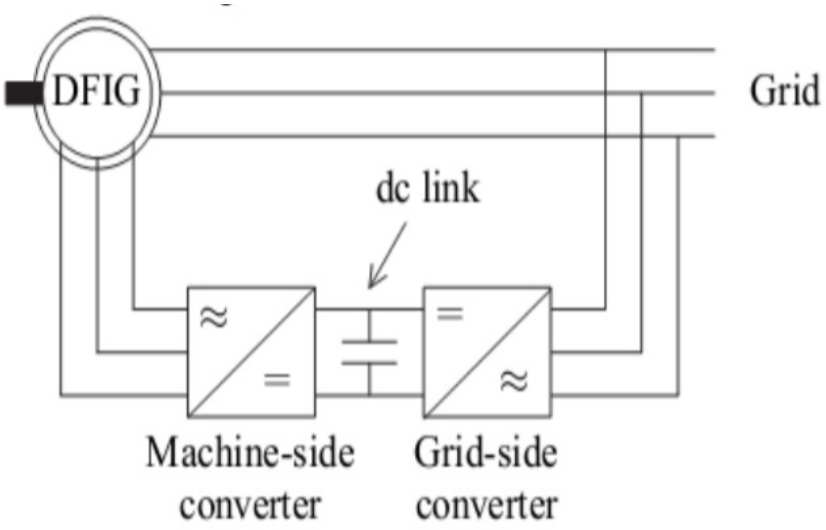

Figure 2.1: DFIG system with a back-to-back converter.

2.2.3 direct current machines

This type of machine is little used in wind energy. The stator in these machines uses a DC source to create a constant magnetic field across the rotor. This field can also be created using permanent magnets. Unlike alternating current machines, it is the stator that acts as the inductor. As a generator, the rotor produces power with a rectified current and is connected to the load via a collector-brush system. These machines are generally expensive and their maintenance is expensive. They are mainly used to charge batteries or in heating applications. On the other hand, it is more common to use a permanent magnet synchronous machine with a simple rectifier to do the same work [24].

2.3 Turbine modelling

The wind energy conversion system is complex because of the multiplicity of existing domains, namely, the aerodynamic, mechanical, and electrical domains. And the factors determining mechanical power, such as wind speed, size, and shape of the turbine. To better show the effect of mechanical speed changes on wind speed, we were interested in modelling the turbine. The turbine to be modeled has three blades of length R mounted on a drive shaft that rotates at $\Omega_{turbine}$ speed and drives a generator (DFIG) with a speed gain multiplier G.

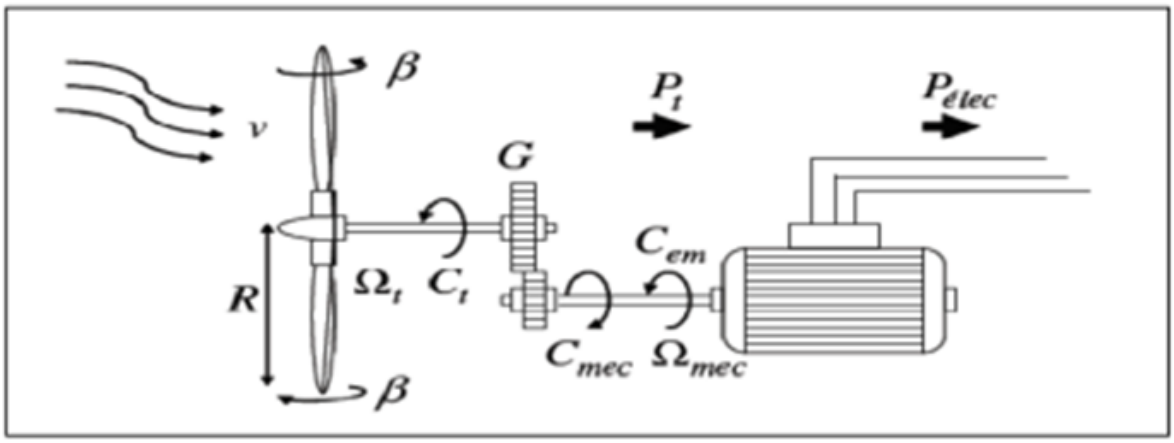

Figure 2.2: Diagram of the wind turbine.

The power of the wind or wind power is defined as follows:

$$P_v = \frac{\rho \cdot S \cdot V^3}{2} \tag{2.1}$$

P_v:the power of the wind [W].

ρ : density of the air $(1.22kg/m3)$.

S : is the circular area swept by the turbine, the radius of the circle is determined by the length of the blade.

V : wind speed [m/s].

The block diagram of the model of the turbine is expressed in 2.3 :

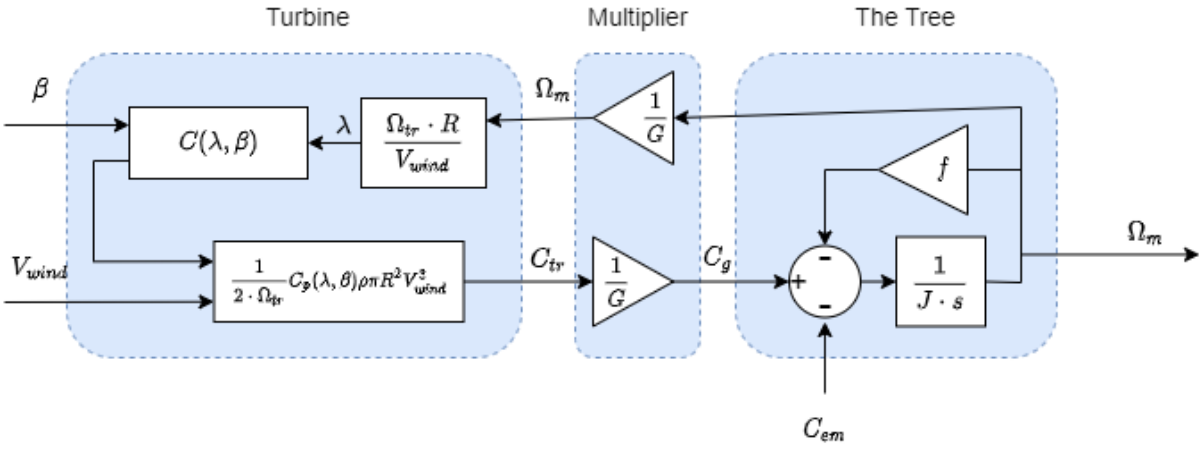

Figure 2.3: Block diagram of the turbine model.

2.3.1 Aerodynamic power

The aerodynamic power appearing at the level of the turbine rotor is then written:

$$P_{aer} = C_p \cdot P_v = C_p(\lambda,\beta) \cdot \frac{\rho \cdot S \cdot V^3}{2} \tag{2.2}$$

And $S = \pi \cdot R^2$

P_{aer}: aerodynamic power [W].

C_p: power coefficient

R: radius of the turbine in meters [m].

λ: speed ratio.

β: angle of the blade orientation [°].

The power coefficient C_P represents the aerodynamic efficiency of the wind turbine. It depends on the characteristic of the turbine. Fig 2.4 represents the variation of this coefficient depending on the speed ratio λ and the angle of the blade orientation β. The speed ratio is defined as the ratio between the linear speed of the blades and the speed of the wind:

$$\lambda = \frac{\Omega_{turbine}.R}{V} \tag{2.3}$$

$\Omega_{turbine}$: the speed of the turbine.

λ: the speed ratio.

R: the radius of the blades.

A turbine is typically characterized by its (λ, β) curve. The formula used in this study is as follows:

$$\begin{cases} A = \frac{1}{\lambda+0.08\cdot\beta} - \frac{0.035}{1+\beta^3} \\ C_P(\lambda,\beta) = 0.5176 \cdot [116 \cdot A - 0.4 \cdot \beta - 5] \cdot \exp(-21.A) + 0.0068.\lambda \end{cases} \tag{2.4}$$

The characteristic of the power coefficient C_P as a function of λ obtained by the above equation and is illustrated by Fig 2.4.

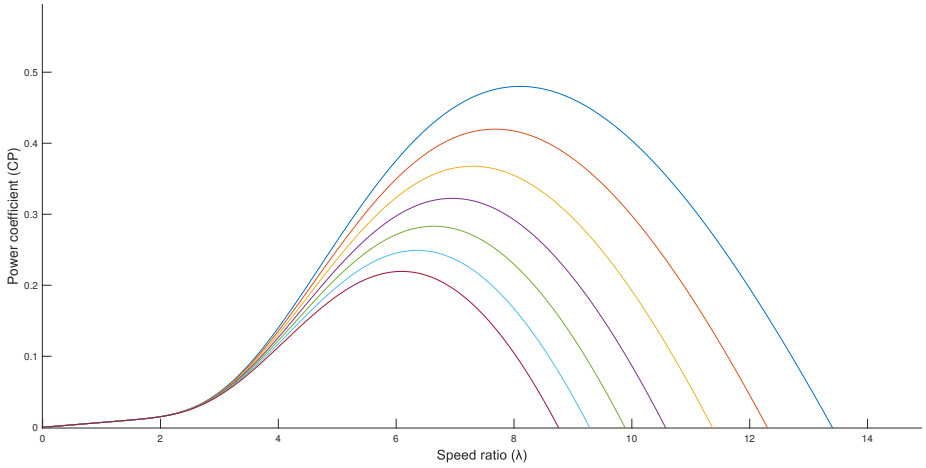

Figure 2.4: Aerodynamic coefficient as a function of turbine speed ratio (λ).

Fig 2.4 represents the function of the power coefficient C_p with respect to the relative speed λ for different pitch angles β. We can notice that the power coefficient goes through a maximum (Cp_{max}= 0.48), for a pitch angle ($\beta = 0^\circ$), a value of the relative speed λ called optimal (λ_{opt}= 8.11).

2.3.2 Aerodynamic torque

So the turbine speed is:

$$\Omega_{turbine} = \frac{\lambda \cdot V}{R} \tag{2.5}$$

Knowing the speed of the turbine, the aerodynamic torque is therefore directly determined by:

$$C_{aer} = \frac{P_{aer}}{\Omega_{turbine}} \cdot C_p(\lambda, \beta) \cdot \frac{\rho \cdot S \cdot V^2}{2} \cdot \frac{1}{\Omega_{turbine}} \tag{2.6}$$

By substitution of $\Omega_{turbine}$ in equation, the expression of the aerodynamic torque will be expressed by:

$$C_{aer} = \frac{1}{2\lambda} \cdot C_p(\lambda, \beta) \cdot \rho \cdot S \cdot V^2 \tag{2.7}$$

2.3.3 Multiplier model

The multiplier adapts the speed of the turbine to the speed of the generator. This multiplier is modelled mathematically by a gain G expressed by the following equations:

$$C_g = \frac{C_{aer}}{G} \tag{2.8}$$

$$\Omega_{turbine} = \frac{\Omega_{mec}}{G} \tag{2.9}$$

C_{aer} : aerodynamic torque of the turbine [Nm].

C_g : the torque resulting from the multiplier.

G : multiplier ratio.

Ω_{mec} : generator speed [rad/s].

$\Omega_{turbine}$: turbine speed [rad/s].

2.3.4 Shaft dynamic equation

The dynamic operation of the generator shaft is expressed by the fundamental equation:

$$J = \frac{J_{turbine}}{G} + J_m \tag{2.10}$$

$$J \cdot \frac{d\Omega_{mec}}{dt} = \sum torques = C_{mec} \tag{2.11}$$

$$C_{mec} = C_g - C_{em} - f \cdot \Omega_{mec} \tag{2.12}$$

J : the total inertia that appears on the generator rotor.

$J_{turbine}$: turbine inertia [kg.m2].

J_m : generator inertia[kg.m2].

C_{mec} : mechanical torque.

C_{em} : electromagnetic torque [Nm].

C_g : the torque resulting from the multiplier.

f : viscous coefficient of friction.

2.4 Variable Speed wind turbine control Strategies

The power produced by a wind turbine depends on the wind speed. In this frame, Fig 2.5 shows the power curve of a 5MW wind turbine at its different operating zones [25].

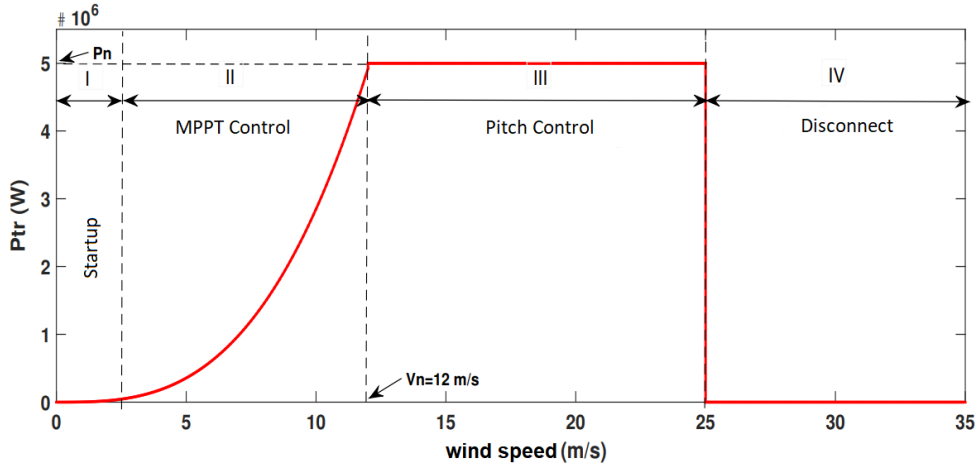

Figure 2.5: Wind turbine operating areas.

- **Zone** I **:** $V_{wind} < 3m/s$

  The wind speed is too low. This causes the turbine to produce a very low energy.

- **Zone II :** $3m/s < V_{wind} < 12m/s$

  The power captured in this zone is maximized by a control strategy called MPPT (Maximum Power Point Tracking) for each wind speed. The curve is characterized by a power proportional to the cube of the speed of the wind. The wind speed increases, until it reaches 12 m/s where the machine reaches its rated power, which in this case is 5MW. The behavior of the wind turbine in this zone is defined by operation at partial load C_p, i.e. below the nominal power. A control strategy is applied in this area. Thus, its main objective is to maximize the energy captured from the wind and minimize the forces undergone by the device training.

- **Zone III :** $12m/s < V_{wind} < 25m/s$

  Beyond a threshold corresponding to the nominal wind speed, the power electrical power is limited to the nominal power of the machine in order to avoid the unhooking of the structure. This is done by the control strategy called ”Pitch control” by acting on the orientation of the blades. The behavior of the wind turbine in this zone, is defined by operation at full load (PC).

► **Zone IV :** $25m/s < V_{wind} < 35m/s$

Wind speeds exceed the trigger speed (≈ 25m/s), which causes the wind turbine to stop with zero power.

2.5 Principle of the MPPT Strategy

The principle of the MPPT Maximum Power Point Tracking strategy consists, for a given blade angle, in adjusting, depending on the wind speed V_{wind}, the rotational speed of the wind turbine to a reference value Ω_t * to maintain a speed relative optimal and therefore a maximum power coefficient Cp_{max}.

$$\Omega_t = \frac{V_{wind} \cdot \lambda_{max}}{R} \tag{2.13}$$

It is the action on the electromagnetic torque (and therefore on the power converted by the generator) that will make it possible to obtain Ω tub and thus maximize the power extracted with the maintenance of Cp_{max}.

2.6 Maximum Power Extraction Technique

The purpose of the MADA variable speed control is to extract the maximum power from the wind turbine. For this, we need an algorithm acting on the set point variables in order to obtain the best possible performance from the device. Through the bibliography study, we have distinguished two families of control structures for the maximization of the extracted power:

✣ MPPT using control engineering.

✣ MPPT without using control engineering.

2.6.1 using control engineering

In the structure shown in Fig 2.6 reference speed is defined as the setpoint to be applied to the electromagnetic torque regulator, to continuously and effectively track the maximum power. The corrector of speed is proportional-integral (PI).

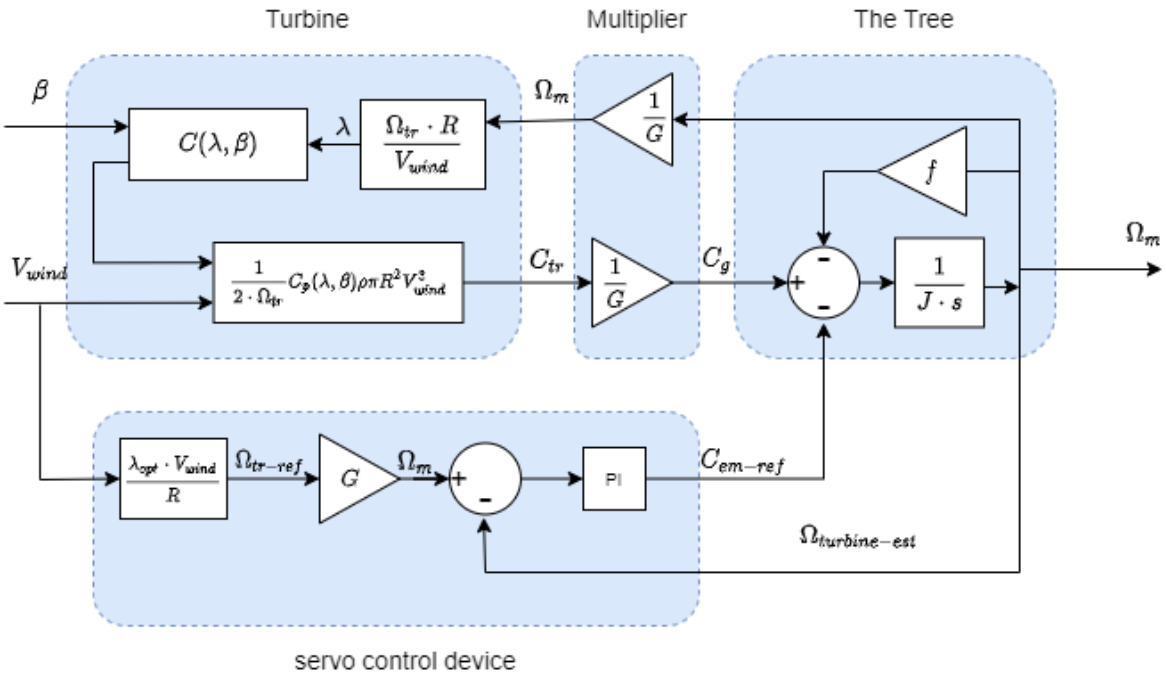

Figure 2.6: diagram Block of extracted power maximization using control engineering.

The following relation gives the reference speed of rotation:

$$\Omega_{m-ref} = \frac{V_{wind}\cdot\lambda_{max}}{R} \tag{2.14}$$

The optimal specific speed therefore makes it possible to establish the optimal relationship between the maximum power and the rotational speed of the reference turbine Ω_{m-ref}. From the characteristic of the power coefficient Equation,that allows to determine the maximum values. The characteristic of the power coefficient $C_p(\lambda,\beta)$, is a function not linear of the specific speed λ and of the angle of orientation β . The optimal operation of the turbine is determined for a power coefficient maximum. It reaches this value for a relative speed $\lambda = \lambda_{max}$=8.11 .

PI Regulator Synthesis

By considering the following system figure 2.7 of the first order, the gains proportional and integral of the PI regulator will be determined: R(s) is the regulator transfer function represented by equation 2.15:

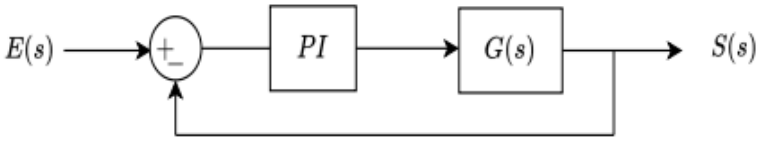

Figure 2.7: PI controller block diagram.

$$R(s) = K_P + \frac{K_i}{s} \tag{2.15}$$

$$G(s) = \frac{k}{1+Ts} \tag{2.16}$$

K: Static gain.

T: Time constant.

The closed-loop transfer function of the system in Figure 2.7 will therefore be:

$$H(s) = \frac{k(K_p s + K_i)}{s(1+Ts) + k(K_p s + K_i)} \tag{2.17}$$

The characteristic function of this system is given by equation 2.18:

$$D(s) = s^2 + \frac{kK_p + 1}{T}s + \frac{kK_i}{T}s \tag{2.18}$$

By identification with the transfer function of a second-order system, with a natural pulsation ω_n and a damping coefficient ξ. The gains of the regulator, are defined as follows:

$$K_p = \frac{2\xi\omega_n T - 1}{k} \tag{2.19}$$

and

$$K_i = \frac{T\omega_n^2}{k} \tag{2.20}$$

However, the association of the various devices constituting the production chain wind turbine, makes the mathematical model more complex. For this, the gains per pole placement (equations 2.19 and 2.20), must be adjusted to produce improved the results. This led us to solve an optimization problem, using meta-heuristics.

2.6.2 without using control engineering

To establish this MPPT control structure without speed control, it is necessary to hypothesize that the wind speed varies very little in steady state (the system is assumed to be in a steady state). In this case, from the dynamic equation of the turbine, we obtain the static equation describing the steady state of the turbine [26], [27]:

$$J\frac{d\Omega}{dt} = C_{mec} = 0 = C_m - C_{em} - C_{visq} \tag{2.21}$$

If we neglect the effect of the viscous torque. We obtain:

$$C_{em} = C_m \tag{2.22}$$

The electromagnetic torque is determined from an estimate of the air-generating torque.

$$C_{em}^* = \frac{C_{are-est}}{G} \tag{2.23}$$

The aerogenerator torque is itself estimated according to the wind speed and the turbine speed

$$C_{are-est} = \frac{P_{are}}{\Omega_{turbine}} = \frac{1}{2} \cdot \rho \cdot \pi \cdot R^2 \cdot C_p(\lambda, \beta) \cdot V_{wind-est}^3 \cdot \frac{1}{\Omega_{turbine-est}} \tag{2.24}$$

An estimate of the turbine speed is calculated from the mechanical speed:

$$\Omega_{turbine-est} = \frac{R \cdot \Omega_{mec}}{G} \tag{2.25}$$

The estimate of the wind speed is then expressed by:

$$V_{wind-est} = \frac{R \cdot \Omega_{turbine-est}}{\lambda} \tag{2.26}$$

From these relations we have:

$$C^*_{em} = \frac{C_p \cdot \rho \cdot \pi \cdot R^5 \cdot \Omega^3_{mec}}{2 \cdot G^3 \cdot \lambda^3} \tag{2.27}$$

To extract the maximum power generated; We must set the speed ratio to λ_{opt} which corresponds to the maximum of the power coefficient C_{Pmax}

The estimated electromagnetic torque must then be set to the following value:

$$C^*_{em} = \frac{C_p \cdot \rho \cdot \pi \cdot R^5 \cdot \Omega^3_{mec}}{2 \cdot G^3 \cdot \lambda^3_{opt}} \tag{2.28}$$

The block diagram representation of the control device is shown in Fig 2.8:

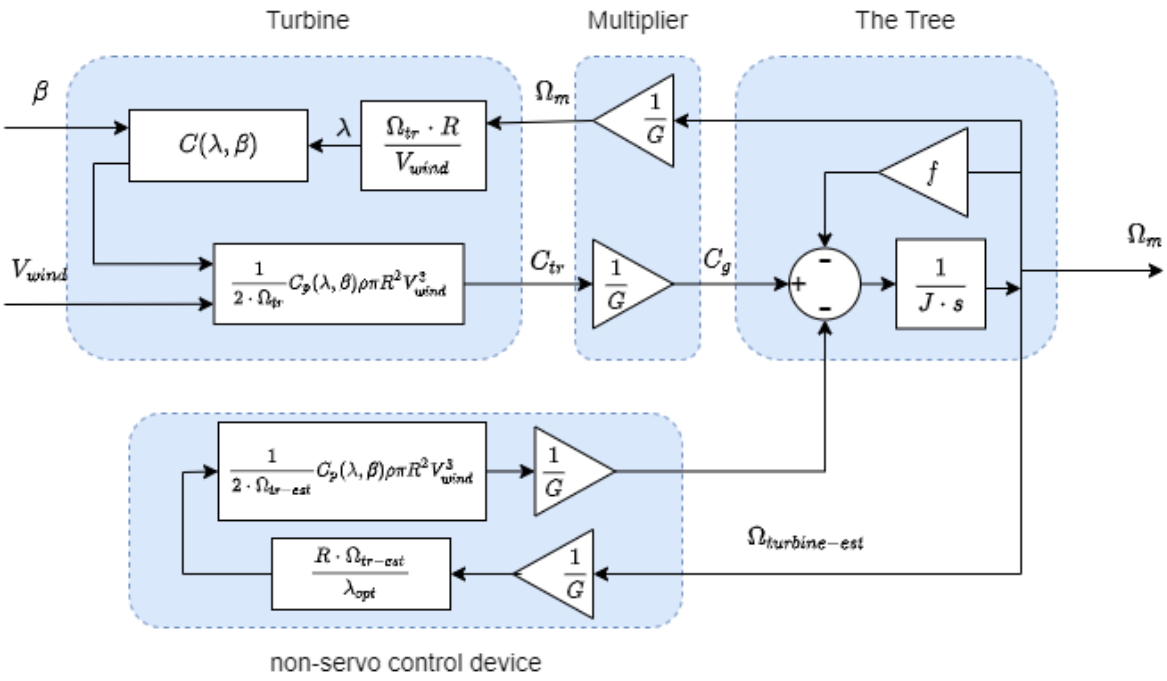

Figure 2.8: Block diagram of the maximization of the power extracted without speed control.

2.7 DFIG three-phase model

The double-fed asynchronous machine can be modeled by six electrical equations and a single mechanical equation that concerns the dynamics of the rotor. As schematically shown in Fig 2.9, The phases are denoted by a_s , b_s , c_s for the stator and a_r , b_r , c_r for the rotor. The electrical angle θ defines the instantaneous relative position between the magnetic axes of the stator and rotor phases [9].

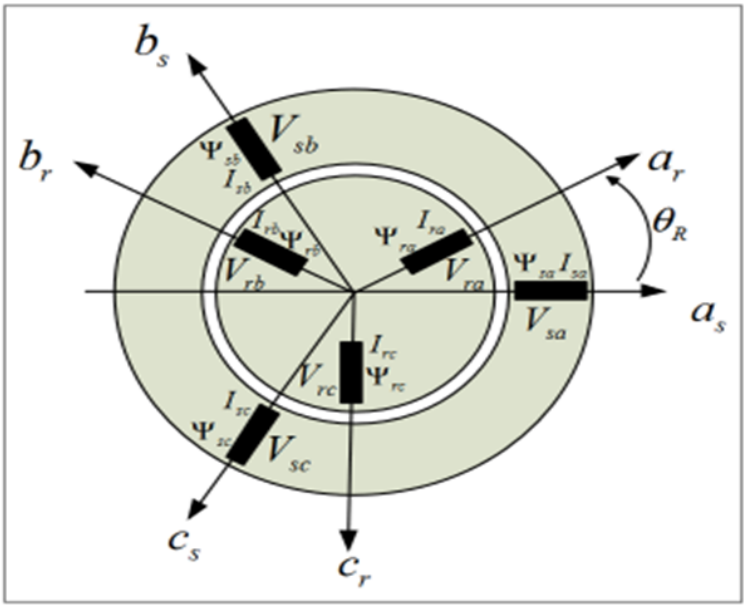

Figure 2.9: Spatial representation of the asynchronous machine in the three-phase frame.

a_s , b_s , c_s : The vectors oriented along the stator windings.

a_r , b_r , c_r: The vectors oriented along the rotor windings.

θ : The position angle between the stator and the rotor.

2.7.1 Voltage equation in the "ABC" plan

The stator and rotor voltage equations can be expressed, using matrix notation, by:

$$\begin{aligned}[V_s] &= [R_s] \cdot [I_s] + \frac{d}{dt}[\Psi_s] \\ [V_r] &= [R_r] \cdot [I_r] + \frac{d}{dt}[\Psi_r]\end{aligned} \tag{2.29}$$

With :

$[V_s] = \begin{bmatrix} V_{sa} \\ V_{sb} \\ V_{sc} \end{bmatrix}$ and $[V_r] = \begin{bmatrix} V_{ra} \\ V_{rb} \\ V_{rc} \end{bmatrix}$: stator and rotor voltages.

$[I_s] = \begin{bmatrix} I_{sa} \\ I_{sb} \\ I_{sc} \end{bmatrix}$ and $[I_r] = \begin{bmatrix} I_{ra} \\ I_{rb} \\ I_{rc} \end{bmatrix}$: stator and rotor currents.

$[\Psi_s] = \begin{bmatrix} \Psi_{sa} \\ \Psi_{sb} \\ \Psi_{sc} \end{bmatrix}$ and $[\Psi_r] = \begin{bmatrix} \Psi_{ra} \\ \Psi_{rb} \\ \Psi_{rc} \end{bmatrix}$: flow vectors.

$$[R_s] = \begin{bmatrix} R_s & 0 & 0 \\ 0 & R_s & 0 \\ 0 & 0 & R_s \end{bmatrix} \text{ and } [R_r] = \begin{bmatrix} R_r & 0 & 0 \\ 0 & R_r & 0 \\ 0 & 0 & R_r \end{bmatrix} : \text{Resistor matrices.}$$

2.7.2 Flux equations in the "ABC" plane

We denote the flow equations in the "ABC" plane by the following expression:

$$\begin{aligned} [\Psi_s] &= [\mathrm{L}_s] \cdot [\mathrm{I}_s] + [\mathrm{L}_m] \cdot [\mathrm{I}_r] \\ [\Psi_r] &= [\mathrm{L}_r] \cdot [\mathrm{I}_r] + [\mathrm{L}_m]^T \cdot [\mathrm{I}_r] \end{aligned} \tag{2.30}$$

With Stator and rotor leakage inductance matrix:

$$[L_s] = \begin{bmatrix} L_{ls} & M_{ss} & M_{ss} \\ M_{ss} & L_{ls} & M_{ss} \\ M_{ss} & M_{ss} & L_{ls} \end{bmatrix} \quad [L_r] = \begin{bmatrix} L_{lr} & M_{rr} & M_{rr} \\ M_{rr} & L_{lr} & M_{rr} \\ M_{rr} & M_{rr} & L_{lr} \end{bmatrix} \tag{2.31}$$

L_{ls} and L_{lr}, respectively the inductances of a phase at the stator and of a phase at the rotor

M_{ss} and M_{rr}, respectively the mutual inductances between two phases of the stator and between two rotor phases,

the matrix of inductors cyclic mutuals between the stator and the rotor:

$$[L_m] = L_{sr} \cdot \begin{bmatrix} cos(p \cdot \theta_r) & cos(p \cdot \theta_r + \frac{2\pi}{3}) & cos(p \cdot \theta_r - \frac{2\pi}{3}) \\ cos(p \cdot \theta_r - \frac{2\pi}{3}) & cos(p \cdot \theta_r) & cos(p \cdot \theta_r + \frac{2\pi}{3}) \\ cos(p \cdot \theta_r + \frac{2\pi}{3}) & cos(p \cdot \theta_r - \frac{2\pi}{3}) & cos(p \cdot \theta_r) \end{bmatrix}$$

p is number of pole pairs of the asynchronous machine.

2.7.3 Mechanical equations of the machine

The electromagnetic torque is given by the following general expression:

$$C_{em} = p\,[\mathrm{I}_s]^T \cdot \frac{d}{d\theta}\left([L_m] \cdot [\mathrm{I}_r]\right) \tag{2.32}$$

2.8 Change frame to the dq plane

2.8.1 Park transformation

The Park transformation consists of transforming the stator and rotor windings into equivalent orthogonal windings, in order to obtain a more mathematical model simple as the physical model of the system.

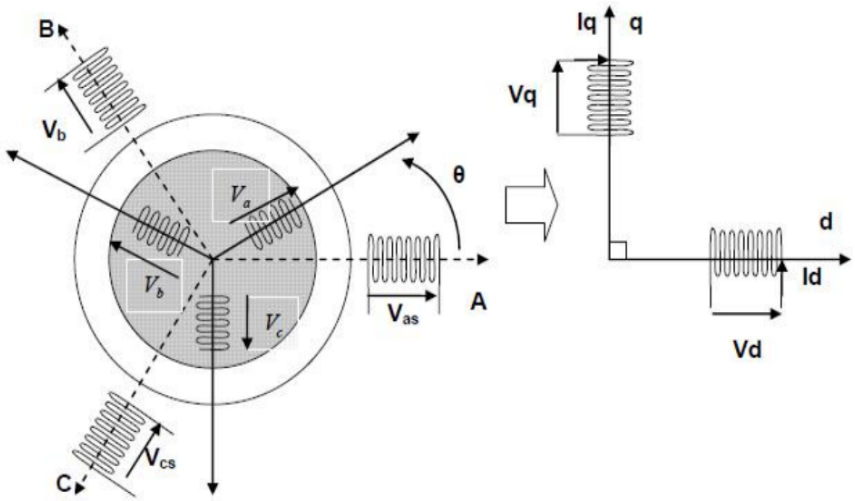

Figure 2.10: DFIG PARK model.

The transformation matrix is defined by:

$$[p(a)] = \sqrt{\frac{2}{3}} \cdot \begin{bmatrix} cos(\alpha) & cos(\alpha - \frac{2\pi}{3}) & cos(\alpha + \frac{2\pi}{3}) \\ -sin(\alpha) & -sin(\alpha - \frac{2\pi}{3}) & -sin(\alpha + \frac{2\pi}{3}) \\ \frac{1}{\sqrt{2}} & \frac{1}{\sqrt{2}} & \frac{1}{\sqrt{2}} \end{bmatrix} \tag{2.33}$$

The angle α is user-selectable and may depend on time. The fact that $[P(\alpha)]$ is orthonormal implies that its inverse is equal to its transpose $[P(\alpha)]^T = [P(\alpha)]^{-1}$.

2.8.2 Voltage equations

$$\begin{cases} V_{sd} = R_s, I_{sd} + \frac{d}{dt}\Phi_{sd} - \omega_s, \Phi_{sq} \\ V_{sq} = R_s, I_{sq} + \frac{d}{dt}\Phi_{sq} + \omega_s, \Phi_{sd} \\ V_{rd} = R_r, I_{rd} + \frac{d}{dt}\Phi_{rd} - \omega_r, \Phi_{rq} \\ V_{rq} = R_r, I_{rq} + \frac{d}{dt}\Phi_{rq} + \omega_r, \Phi_{rd} \end{cases} \tag{2.34}$$

With:

ω_s : The rotational speed of the electromagnetic field of the stator.

$\omega_r = \omega_s - \omega_R$: Rotor rotational speed.

2.8.3 Flow equations

$$\begin{cases} \Phi_{sd} = L_s \cdot I_{sd} + M_{sr} \cdot I_{rd} \\ \Phi_{sq} = L_s \cdot l_{sq} + M_{sr} \cdot I_{rq} \\ \Phi_{rd} = L_r \cdot I_{rd} + M_{rs} \cdot I_{sd} \\ \Phi_{rq} = L_r \cdot I_{rq} + M_{rs} \cdot I_{sq} \end{cases} \tag{2.35}$$

With:

$L_s = I_s + M_s$: Stator cyclic inductance.

$M_{sr} = 3M/2$: Cyclic mutual inductance.

$L_r = I_r + M_r$: Rotor cyclic inductance.

2.8.4 Electromagnetic torque equations

The electromagnetic torque of the asynchronous machine can be expressed by the following expression:

$$C_{em} = p\frac{M_{sr}}{L_r}\left(\Phi_{sd} \cdot I_{rq} - \Phi_{sq} I_{rd}\right) \tag{2.36}$$

2.9 DFIG Vector Command

The vector control technique is based on a control law leading to an adjustment characteristic similar to that of a separately excited DC machine. For the case of the vector control of the DFIG, it will be a question of controlling the energy exchanges and in particular, the transfers of active and reactive powers sent to the network [28]. For the case of this work, the frame (d, q) is keyed to the stator flux. The control concerns, of course, the powers returned to the network, therefore on the side of the stator (generator convention) and consequently the rotor will be considered as a control device (receiver convention).

2.10 Principle of flux-oriented control

In this work, the development of the DFIG oriented stator flux vector control is exposed. Thus, as shown in Fig 2.11 the flux will be stalled on the "d" axis and the stator voltage on the "q" axis, this last constraint is favourable to have a control model simplified [29] [17][30][9][31][32].

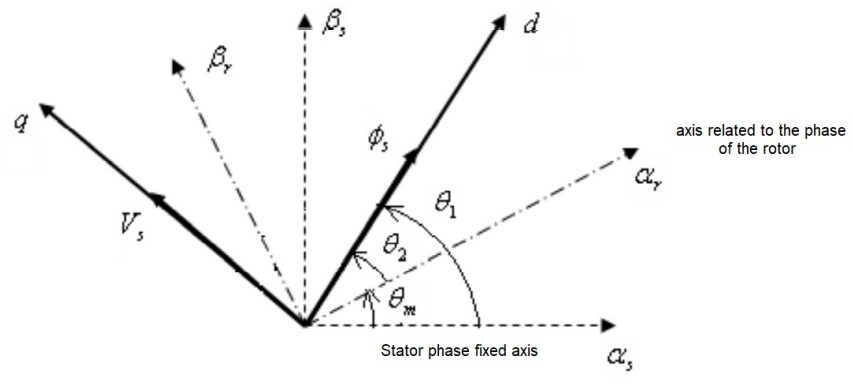

Figure 2.11: Voltage and stator flux vectors in the chosen axis system.

The equation of the electromagnetic torque then becomes:

$$C_{em} = P \cdot \frac{M}{L_s} \cdot I_{rq} \cdot \phi_{sd} \tag{2.37}$$

Assuming that the network to which the DFIG is connected is stable, the flux ϕ_{sd} then becomes constant. The choice of this reference makes the electromagnetic torque produced by the machine and consequently the active power solely dependent on the rotor current of axis "q" [33][34]. In the three-phase reference, the stator voltages are expressed by the following expression:

$$[V_s] = [R_s]\,[i_s] + \frac{d}{dt}\,[\psi_s] \tag{2.38}$$

"R_s" being negligible for high power machines used in wind turbines, the expression of the stator voltage then becomes:

$$V_{sd} = \frac{d\phi_s}{dt} \tag{2.39}$$

In the same frame of reference and on the assumption that the stator flux is constant thanks to a supply by a stable network, the voltage equations will be expressed by:

$$\begin{cases} V_{sd} = 0 \\ V_{sq} = V_s = \omega_s \cdot \phi_{sd} = \omega_s \cdot \phi_s \end{cases} \tag{2.40}$$

Using the above simplifications, the flux equations will be expressed as follows:

$$\begin{cases} \phi_s = L_s \cdot I_{sd} + M_{sr} \cdot I_{dr} \\ 0 = L_s \cdot I_{sq} + M_{sr} I_{qr} \end{cases} \tag{2.41}$$

2.10.1 Relations between stator and rotor currents

From the equations of the direct and quadrature component of the stator flux (2.41), we can write the equations relating the stator currents to the rotor currents as follows:

$$\begin{cases} I_{ds} = \frac{\phi_s}{L_s} - \frac{M_{sr}}{L_s} I_{dr} \\ I_{qs} = -\frac{M_{ss}}{L_s} I_{qr} \end{cases} \tag{2.42}$$

2.10.2 Expression of the active and reactive powers in the synchronous frame

In any two-phase frame, the stator active and reactive powers of an asynchronous machine are written [35] [36]:

$$\begin{cases} P_s = \frac{3}{2}(V_{ds} I_{ds} + V_{qs} I_{qs}) \\ Q_s = \frac{3}{2}(V_{qs} I_{ds} - V_{ds} I_{qs}) \end{cases} \tag{2.43}$$

By adapting these equations to the system of axes (d, q) chosen, the model of the DFIG in the steady state gives:

$$\begin{cases} P_s = -\frac{3}{2} V_s I_{qs} \\ Q_s = -\frac{3}{2} V_s I_{ds} \end{cases} \tag{2.44}$$

By replacing I_{ds} and I_{qs} by their expressions given by equation (2.42), we obtain the following expressions for the active and reactive powers:

$$\begin{cases} P_s = \frac{3}{2} V_s \cdot \frac{M_{sr}}{L_s} I_{qr} \\ Q_s = -\frac{3V_s\phi_s}{2L_s} + \frac{3V_s M_{sr}}{2L_s} I_{dr} \end{cases} \tag{2.45}$$

From expression (2.40) we can write:

$$\phi_s = \frac{V_s}{\omega_s} \tag{2.46}$$

$$Q_s = -\frac{3V_s^2}{2L_s\omega_s} + \frac{3V_s M_{sr}}{2L_s} I_{dr} \tag{2.47}$$

Taking into account the reference chosen and the approximations made and if we consider the magnetizing inductance M_{sr} as constant, the system obtained proportionally links the active power to the rotor current of axis "q" and the reactive power to the current rotor axis "d" to the constant $\frac{V_s^2}{L_s \times \omega_s}$ close to imposed by the network.

2.10.3 Expressions of rotor voltages as a function of rotor currents

The rotor fluxes are expressed as a function of the rotor currents, after having replaced the stator currents by their expressions, as follows:

$$\begin{cases} \Phi_{dr} = \left(L_r - \frac{M_{sr}^2}{L_s}\right) I_{dr} + \frac{M_{sr} V_s}{\omega_s L_s} \\ \Phi_{qr} = \left(L_r - \frac{M_{sr}^2}{L_s}\right) I_{qr} \end{cases} \tag{2.48}$$

These expressions for the "d" and "q" axis rotor fluxes are then integrated into the expressions for the two-phase rotor voltages of equation (2.39). We then obtain:

$$\begin{cases} V_{dr} = R_r I_{dr} + \left(L_r - \frac{M_{sr}^2}{L_s}\right) \frac{d}{dt} I_{dr} + g\omega_S \left(L_r - \frac{M_{sr}^2}{L_s}\right) I_{qr} \\ V_{qr} = R_r I_{qr} + \left(L_r - \frac{M_{sr}^2}{L_s}\right) \frac{d}{dt} I_{qr} + g\omega_s \left(L_r - \frac{M_{sr}^2}{L_s} I_{dr}\right) + g\omega_S \frac{M_{sr} V_s}{\omega_s L_s} \end{cases} \tag{2.49}$$

We have $\sigma = 1 - \frac{M_{sr}^2}{L_r . L_s}$ and therefore:

$$\begin{cases} V_{dr} = R_r I_{dr} + L_r \sigma \frac{dI_{dr}}{dt} - g\omega_s L_r \sigma I_{qr} \\ V_{qr} = R_r I_{qr} + L_r \sigma \frac{dI_{qr}}{dt} + g\omega_s L_r \sigma I_{dr} + g\frac{M_{sr} V_s}{L_s} \end{cases} \tag{2.50}$$

2.11 Conclusion

In this chapter, we explore different types of machines, then the principle of operation of the MPPT, and the techniques for extracting maximum power.and we presented the complete model of the double-fed asynchronous machine in Park's benchmark related to the rotating field.

Chapter 3

PRESENTATION OF THE STRUCTURE OF FUZZY MODELS TAKAGI-SUGENO

3.1 Introduction

The use of multi models make it possible to obtain a mathematical model, representing the behavior of the nonlinear system, in a form broken down by subsets linear. Therefore, the system becomes less complex to perform control and stability analysis. In the domain of control, several strategies use the variables of the state vector or the synthesis of the control law. However, in practical terms, these variables may not be accessible to measurement. In this case, the observer is used to replace expensive or difficult-to-maintain sensors to provide an estimate of the current value of the state, based on system inputs and outputs.

On the other hand, fuzzy systems of the Takagi-Sugeno type are widely used, so both in the analysis and in the synthesis of the control law, with reduction of the conservatism of the synthesis conditions. They are represented as a set of simple structure sub-models [37][38].

3.2 Presentation of the structure of fuzzy models Takagi-Sugeno

A nonlinear system can be modeled in the general form given by equations 3.1:

$$\begin{cases} \dot{x}(t) = f(x(t)) + g(x(t))u(t) \\ y(t) = \varphi(x(t)) + m(x(t))u(t) \end{cases} \tag{3.1}$$

Where $x(t) \in R^n$ is the state vector, $u(t) \in R^m$ is the input vector with which the system can be controlled and $y(t) \in R^q$ is the output vector.

$f(x(t))$, $g(x(t))$, $(x(t))$ and $m(x(t))$ are nonlinear functions with appropriate dimensions.

Since their introduction in 1985, Takagi-Sugeno type fuzzy models are described by a set of **If – Then fuzzy rules** [39].

The fuzzy Takagi-Sugeno model equations 3.2 can be constructed by a set of fuzzy rules R_i of **If-Then** type, representing the input/output relations of a nonlinear system. This design must ensure the accuracy of the reproduction of the behavior of the system over a wide operating range. The i^{th} rule of the fuzzy model is written in the following form:

If $z_1(t)$ is F_{1i} and ... and **If** $z_g(t)$ is F_{gi} **Then**

$$\begin{cases} \dot{x}(t) = A_i x(t) + B_i u(t) \\ y(t) = C_i x(t) + D_i u(t) \end{cases} \quad i = 1, \ldots, r. \tag{3.2}$$

where r is the number of fuzzy rules,

A_i, B_i, C_i and D_i are the appropriate matrices of the subsystems, where $A_i \in R^{n\times n}$ is here state matrix, $B_i \in R^{n\times m}$ is the control matrix, $C_i \in R^{q\times n}$ is the matrix of observation and $D_i \in R^{q\times m}$ is the forward transmission matrix.

F_{gi} is the fuzzy set and $z_1(t)...z_g(t)$ are the premise variables.

A fuzzy model of the Takagi-Sugeno type is composed of a finite set of models linear interconnected through nonlinear functions. The fuzzy model of the resulting system appears, as a weighted average of the local models, in the following compact (defuzzified) form:

$$\begin{cases} \dot{x}(t) = \sum_{i=1}^{r} \mu_i(z(t)) \left(A_i x(t) + B_i u(t)\right) \\ y(t) = \sum_{i=1}^{r} \mu_i(z(t)) \left(C_i x(t) + D_i u(t)\right) \end{cases} \tag{3.3}$$

Where $i = 1, ..., r,\ z(t) = [z_1(t)\ z_2(t)\ ...\ z_g(t)]$.

Let $F_{ij}(z_j(t))$: the membership values of the variables of the premises $z_j(t)$ in the fuzzy subsets F_{ij} . The barycentric deffuzification of the system (3.2), is obtained by setting:

$w_i(z(t)) = \Pi_{j=i}^{p} F_{ij}(z_j(t)) > 0$ and considering the following membership functions:

$$\mu_i(z(t)) = \frac{w_i(z(t))}{\sum_{i=1}^{r} w_i(z(t))} \tag{3.4}$$

and $\forall t \geq 0$, then

$$\begin{cases} \sum_{i=1}^{r} w_i(z(t)) > 0 \\ w_i(z(t)) \geq 0 \end{cases} \tag{3.5}$$

For an i^{th} rule, the membership function $\mu_i(z(t))$ indicates the degree of activation of the i^{th} associated local model, verifying the property of the following convex sum:

$$\begin{cases} \sum_{i=1}^{r} \mu_i(z(t)) = 1 \\ 0 \leq \mu_i(z(t)) \leq 1 \end{cases} \tag{3.6}$$

3.3 Modelling the fuzzy of Takagi-Sugeno

The modeling of the fuzzy system defined by the system of equations (3.3), is established from the data on the model. It can be described according to these three approaches.

3.3.1 Identification of the Takagi-Sugeno model

This method allows to obtain a Takagi-Sugeno fuzzy model from the I/O data obtained by measurements of the real system. To and effect, this method is used, in absence of the analytical model of the nonlinear system [39] [40] [27]. The fuzzy dynamic model of the Takagi-Sugeno type includes the parameters of the antecedent and the consequent for each of the rules. The estimation of the parameters of each subsystem is defined by the techniques method based on numerical optimization algorithms, for the minimization of quadratic error between the output of the estimated Takagi-Sugeno fuzzy model and that of the model measure

3.3.2 Linearization of the Takagi-Sugeno model

In the presence of the analytical form of the nonlinear model of a physical process, the linearization method consists in linearizing the preestablished nonlinear system around several operating points. Obtaining a T-S structure, is achieved in this case, by the interconnection of these models, using carefully defined nonlinear membership functions (Gaussian, triangular, trapezoidal,. . . etc) [38] [41]. Consider the following nonlinear system:

$$\begin{cases} \dot{x}(t) = f(x(t), u(t)) \\ y(t) = g(x(t), u(t)) \end{cases} \tag{3.7}$$

Where $f \in R^n, g \in R^P$ are continuous nonlinear functions, $x(t) \in R^n$ is the vector state and $u(t) \in R^m$is the control vector. The representation of the nonlinear system (3.7) by a fuzzy model Takagi-Sugeno, is constituted of several local models, in linear or affine form. These are obtained by linearizing the nonlinear system, around an arbitrary operating point $(x_i, u_i) \in R^n \times R^m$. The fuzzy Takagi-Sugeno representation by linearization is as follows:

$$\begin{cases} \dot{x}_m(t) = \sum_{i=1}^{r} \mu_i(z(t)) \left(A_i x_m(t) + B_i u(t) + D_i\right) \\ y_m(t) = \sum_{i=1}^{r} \mu_i(z(t)) \left(C_i x_m(t) + E_i u(t) + N_i\right) \end{cases} \tag{3.8}$$

with

$$A_i = \left.\frac{\partial f(x,u)}{\partial x}\right|_{\substack{x = x_i \\ u = u_i}}, \quad B_i = \left.\frac{\partial f(x,u)}{\partial u}\right|_{\substack{x = x_i \\ u = u_i}}$$

$$C_i = \left.\frac{\partial g(x,u)}{\partial x}\right|_{\substack{x = x_i \\ u = u_i}}, \quad E_i = \left.\frac{\partial g(x,u)}{\partial u}\right|_{\substack{x = x_i \\ u = u_i}}$$

$$D_i = f(x_i, u_i) - A_i x - B_i, \quad N_i = g(x_i, u_i) - C_i x - E_i u$$

The number of local models $'r'$ obtained, depends on the desired precision of the modeling, the complexity of the nonlinear system and the choice of the structure of the activation functions. It must also satisfy the properties of the convex sum [42].

3.3.3 Breakdown of the Takagi-Sugeno model

The objective of this approach is to find a global sector by decomposition into nonlinear sectors of a pre-established nonlinear model, which satisfies the conditions of the system $a_1x(t) \leq f(x(t), u(t)) \leq a_2x(t)$. This method makes it possible to pass from a nonlinear analytical model, to a model Takagi-Sugeno, by representing the nonlinear model exactly in a form of state space, also called approach by non-linear sectors. Unlike the two approaches cited above, the Takagi-Sugeno type representation of the nonlinear model is not approximate. For this, the model given by the system of equations 3.7, is described by an exact conception represented in a space compact state variables. However, it is not always easy to find a sector global for the nonlinear system. To this end, the local sector provides better solutions to represent this type of model (see. figure 3.1) [43].

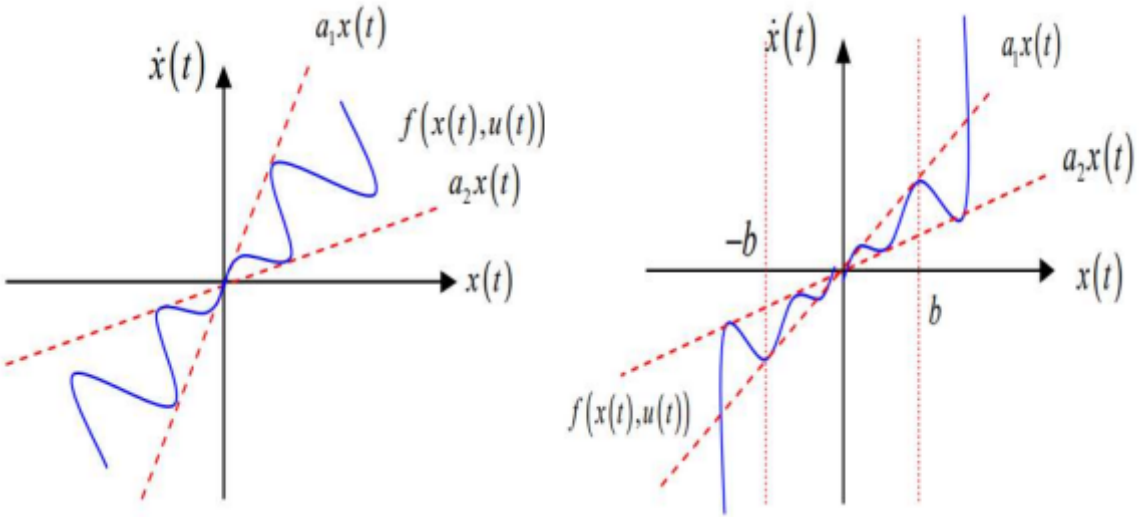

Figure 3.1: Global and local nonlinear sectors

The Takagi-Sugeno models obtained from a decomposition into nonlinear sectors, have advantages from the point of view of precision and knowledge of the membership functions that ensure the interconnection of local models. Note that the approach by non-linear sectors, makes it possible to associate an infinity of Takagi-Sugeno models for a nonlinear system, according to the cutting of the nonlinearities carried out. A systematic approach to dividing into non-linear sectors [44], is based on the following lemma:

Lemma 1 Let $z(t) = f(x(t))$: $R \rightarrow R$ be a bounded function for all $x \in [ab]$, then there exist two functions $\mu_1(z(t))$ and $\mu_2(z(t))$ as well as two real numbers α and β such that [44]:

$$z(t) = \alpha\mu_1(z(t)) + \beta\mu_2(z(t)) \tag{3.9}$$

with

$$\mu_1(z(t)) + \mu_2(z(t)) = 1, \mu_1(z(t)) \geq 0, \mu_2(z(t)) \geq 0 \tag{3.10}$$

Proof Consider the function $f(x(t))$ bounded such that $\alpha \leq z(t) \leq \beta$. We can then always write:

$$z(t) = \alpha\mu_1(z(t)) + \beta\mu_2(z(t)) \tag{3.11}$$

with $\alpha = min(z(t))$ and $\beta = max(z(t))$,

$$\mu_1(z(t)) = \frac{z(t) - \alpha}{\beta - \alpha} \text{ and } \mu_2(z(t)) = \frac{\beta - z(t)}{\beta - \alpha}$$

Exemple Consider the autonomous nonlinear system described by the following equation:

$$\dot{x}(t) = x(t) \cdot \sin(x(t)) \tag{3.12}$$

Let $z(t) = sin(x(t))$, where $z(t)$ is continuous and bounded by $[-11]$ then: $min(z(t)) = -1$ and $max(z(t)) = 1$. Therefore, the membership functions can be calculated as follows:

$$\begin{cases} F_{11}(z(t)) = \frac{z(t)+1}{2} \\ F_{12}(z(t)) = \frac{1-z(t)}{2} \end{cases} \tag{3.13}$$

According to **Lemma 3.1**, we can write:

$$z(t) = \frac{z(t)+1}{2} \times (1) + \frac{1-z(t)}{2} \times (-1)$$

$$z(t) = F_{11}(z(t)) \cdot (1) + F_{12}(z(t)) \cdot (-1) \tag{3.14}$$

where

$$F_{11}(z(t)) + F_{12}(z(t)) = 1 \tag{3.15}$$

The nonlinear system (3.12) can be represented by the set of fuzzy rules following:

R_1 : If $z(t)$ is F_11 then $\dot{x}(t) = A_1x(t))$

R_2 : If $z(t)$ is F_12 then $\dot{x}(t) = A_2x(t)$

Thus, the Takagi-Sugeno model is given in its compact form by:

$$\dot{x}(t) = \sum_{i=1}^{r} \mu_i(z(t))A_ix(t) \tag{3.16}$$

With: $A_1 = 1$ and $A_2 = -1$ Figure (3.2) shows the identical behavior of the systems fuzzy and real of the example cited.

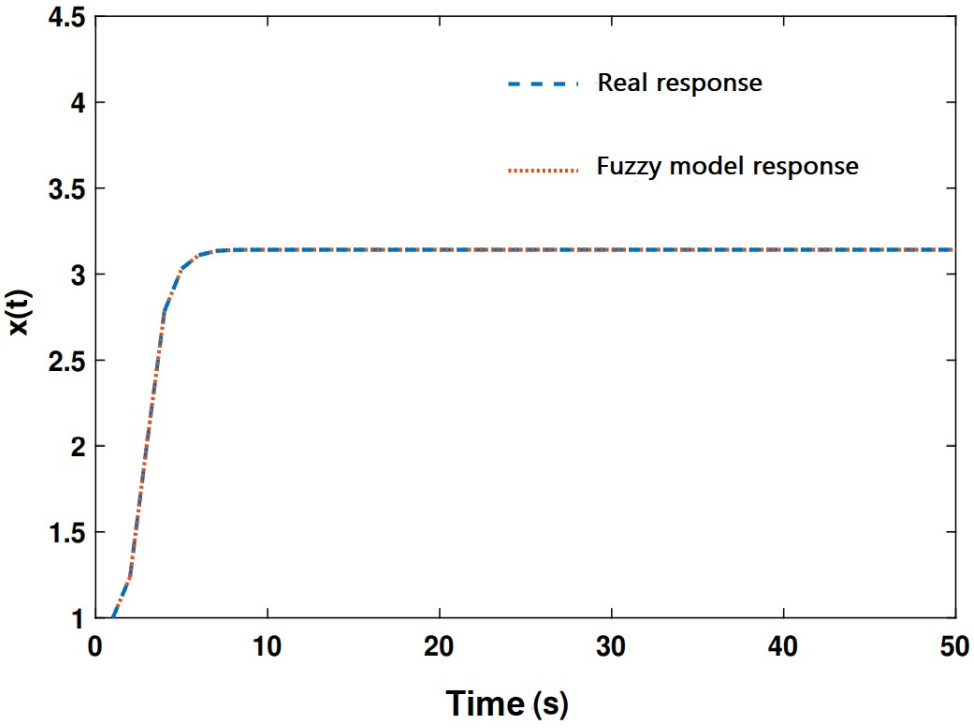

Figure 3.2: Responses of the fuzzy and real systems of the example

3.4 Stability of Takagi-Sugeno fuzzy models

The stability of nonlinear systems obtained by a fuzzy model T-S, has made the subject of much work. The analysis of the stability and the synthesis of the control law of these models are mainly based on Lyapunov's theory [45]. the central paradigm of this theory, is based on a fundamental physical observation of the behavior of the dynamical system, from the point of view of its total energy. If this energy (being generally a scalar), is continuously dissipated, we speak then a dissipative system. In this case, we can hope that the system tends towards a balance point. For this purpose, the use of the candidate Lyapunov function is a distance measure, between the state variables and the equilibrium point. The difficulty of this method lies in the determination of this function. However, the functions of Lyapunov exist in the form of two large families: quadratic functions and not quadratic. Quadratic functions make use of restrictive assumptions and produce sufficient stability conditions, reduced to inequality problems linear matrix (LMI)[46]. Therefore, they can be solved effectively in practice by convex programming techniques. A few reminders about the LMIs, are presented in appendix B. Consider an autonomous Takagi-Sugeno system, represented by:

$$\dot{x}(t) = \sum_{i=1}^{r} \mu_i(z(t)) \left(A_i x(t) + B_i u(t)\right) \tag{3.17}$$

Theorem 1 The system (3.17) is said to be asymptotically stable [38], if and only if it exists a matrix $P \in R^{n\times n}$ symmetric and positive definite verifying the following LMI:

$$A_i^T P + P A_i < 0 \quad i = 1, \ldots, r \tag{3.18}$$

Proof This condition relies on the choice of a quadratic candidate function of Lyapunov (equation 3.19)

$$V(x(t)) = x(t)^T P x(t) \tag{3.19}$$

Where $P = P^T > 0$ The Takagi-Sugeno fuzzy system (3.17) is stable if $\dot{V}(x(t)) < 0$ holds, when the conditions sufficient of Theorem 1 are

$$\dot{V}(x(t)) = \dot{x}(t)^T P x(t) + x(t)^T P \dot{x}(t) < 0 \tag{3.20}$$

3.4.1 Stabilization of Takagi-Sugeno fuzzy models by state feedback

Stability analysis and design technique of T-S fuzzy controllers, are based on work initiated by Tanaka in 1992 [47]. Among which may be mentioned stabilization by state feedback, where the most common are based on the control law

PDC type [48][49]. This procedure (PDC), is a fuzzy combination which defines a control law linear to each sub-model (see. figure 3.2). The closed-loop stability of the whole is guaranteed by means of a common Lyapunov function. The resulting control law is generally nonlinear. The consequence part of each local regulator uses a control gain by state feedback. The general structure of the controller of the i^th rule is then the following: Where Ki are the state feedback gains. The inference of the global fuzzy regulator is given by:

$$u(t) = -\frac{w_i(z(t))K_i x(t)}{\sum_{i=1}^{r} w_i(z(t))} = -\sum_{i=1}^{r} \mu_i(z(t))K_i x(t), i = 1, \ldots, r \tag{3.21}$$

The fuzzy regulator shares the same number of fuzzy rules, with the same sets fuzzy than those of the Takagi-Sugeno fuzzy model.

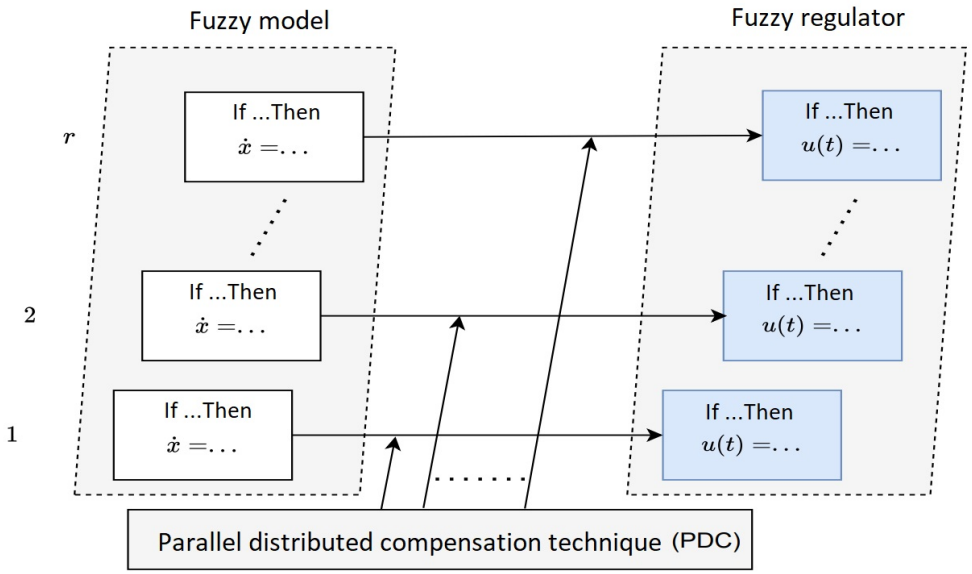

Figure 3.3: Compensation technique.

Stability conditions

Various problems of analysis and synthesis of the control law of nonlinear systems can be reduced to a few

standard optimization problems convex or quasi-convex, using Linear Matrix Inequalities (LMIs) [48] [50]. The convexity of an optimization problem has a double advantage:

- Calculation times are reasonable
- There is no local minimum of the cost function to be optimized. The result obtained corresponds to a unique global minimum.

The stabilization of Takagi-Sugeno fuzzy models by a PDC control law, is based on the Lyapunov function, to ensure the convergence of the closed-loop fuzzy model. In the occurrence, the determination of the state feedback gains corresponds to each model local composing the Takagi-Sugeno model. Thus, from such a function, we can find a positive definite matrix P common between all local closed-loop models.
By substituting equation (3.21) into equation (3.17), the Takagi-Sugeno fuzzy model obtained [51] in a closed loop, takes the following form:

$$\dot{x}(t) = \sum_{i=1}^{r}\sum_{j=1}^{r} \mu_i(z(t))\mu_j(z(t)) \left(A_i - B_i K_j\right) x(t) \tag{3.22}$$

By setting, $G_{ij} = (A_i - B_i K_j)$, equation (3.22) can be rewritten in the following form:

$$\dot{x}(t) = \sum_{i=1}^{r}\sum_{j=1}^{r} \mu_i(z(t))\mu_j z(t)) G_{ij} x(t) + 2\sum_{i=1}^{r}\sum_{i<j} \mu_i(z(t))\mu_j z(t)) \left(\frac{G_{ij}+G_{ji}}{2}\right) x(t) \tag{3.23}$$

The following theorem gives the stabilization conditions of the complete system.

Theorem 2 The closed-loop system (3.22) is asymptotically stable [38], if it exists a matrix $P > 0$ positive definite such that

$$G_{ii}^T P + P G_{ii} < 0, i = 1, \ldots, r \tag{3.24}$$

$$\left(\frac{G_{ij}+G_{ji}}{2}\right)^T P + P\left(\frac{G_{ij}+G_{ji}}{2}\right) \leq 0, i < j \leq r \tag{3.25}$$

For all i and j except the pairs (i, j) such that $\mu_i(z)j(z) = 0$.
The stability conditions given by equations (3.24) and (3.25) are conservative since they require the stability of all the dominant and crossed models.

Conditions of relaxed stability

If the number of rules r is large enough, it is sometimes difficult to find the common matrix P, to satisfy the conditions of Theorems 3.1 and 3.2. In this case, new stability conditions aim to relax the conditions of the theorems 1 and 2 [38]. The new conditions for the synthesis of the control law PDC, could be obtained and are summarized by the following theorem:

Theorem 3 The Takagi-Sugeno fuzzy model (3.22) is asymptotically stable [49], via the PDC command (3.21), if and only if there exists a common matrix $P > 0$, a matrix common $Q \geq 0$ and matrices Ki such that For all i and j except the pairs (i, j) such that $\mu_i(z)\mu_j(z) = 0$. s being the maximum number of local models activated simultaneously.

To further reduce the degree of conservatism of the results of Theorem 3, relaxed stability conditions have been proposed in the following theorem

$$G_{ii}^T P + P G_{ii} + (s-1)Q < 0, i = 1, \ldots, r \tag{3.26}$$

$$\left(\frac{G_{ij} + G_{ji}}{2}\right)^T P + P\left(\frac{G_{ij} + G_{ji}}{2}\right) - Q \leq 0, i < j \leq s \tag{3.27}$$

For all i and j except the pairs (i, j) such that $\mu_i(z)\mu_j(z) = 0$

s being the maximum number of local models activated simultaneously.

To further reduce the degree of conservatism of the results of Theorem 3, Relaxed stability conditions have been proposed in the following theorem.

Theorem 4 If there exists a symmetric matrix $P > 0$, matrices Q_{ij} and matrices K_i [52], who verify:

$$G_{ii}^T P + P G_{ii} + Q_{ii} < 0, i = 1, \ldots, r \tag{3.28}$$

$$\left(\frac{G_{ij} + G_{ji}}{2}\right)^T P + P\left(\frac{G_{ij} + G_{ji}}{2}\right) + Q_{ij} \leq 0, i < j \leq r \tag{3.29}$$

$$\begin{bmatrix} Q_{11} \\ \cdots \\ Q_{1r} \\ \vdots \\ \ddots \\ \vdots \\ Q_{1r} \\ \cdots \\ Q_{rr} \end{bmatrix} > 0 \tag{3.30}$$

For all i and j except the pairs (i, j) such that $\mu_i(z)\mu_j(z) = 0$, system (3.24) is globally asymptotically stable.

The two theorems 3 and 4 guarantee the global stability of the system (3.22). In order to guarantee other control performance, such as response time, constraints on input/output control, have been proposed in the following theorem, considering a certain rate of decrease (delay rate).

Decline rate

Theorem 5 The Takagi-Sugeno fuzzy model (3.22) is globally exponentially stable [53], via the PDC command (3.21) with a decay rate at least equal to α. If he exists a common matrix $P > 0$, a matrix $Q \geq 0$, a scalar α≥0and matrices K_i which satisfy

$$G_{ii}^T P + P G_{ii} + (s-1)Q + 2\alpha s P < 0, i = 1, \ldots, r \tag{3.31}$$

$$\left(\frac{G_{ij} + G_{ji}}{2}\right)^T P + P\left(\frac{G_{ij} + G_{ji}}{2}\right) - Q + 2\alpha P \leq 0, i < j \leq s \tag{3.32}$$

For all i and j except the pairs (i, j) such that $\mu_i(z)j(z) = 0$

α represents the growth rate of the quadratic Lyapunov function to be maximized.

Obtaining the fuzzy regulator PDC, therefore consists in determining the gains of state feedback, for each local model $(Ki, i = 1, ..., r)$, satisfying the conditions stabilization for a positive definite matrix P. These conditions are formulated in LMIs, from a change of variable $X = P^{-}1$ and $K_i = M_i^P - 1$ [54] [55]. Other methods are used to determine the positive definite matrix P and the state return matrices K_i based, that is:

- on the synthesis of the control law by placement of poles, for which a satisfactory transfer function of the system, can be guaranteed by confining its poles in a prescribed region [56].
- on the optimal control, by solving a reduced order Riccati equation.

The calculation of the PDC control law gains used in our work comes from the transformation of the conditions of the theorems cited above (1, 3.2. up to 3.5), into aequivalent problem of LMIs.

In addition, another control law is inspired by the following PDC control on the output return

3.4.2 Stabilization of Takagi-Sugeno fuzzy models by output feedback

Mathematical representation in the form of evolution of internal variables state, requires knowledge of all the components of the state vector.

Generally, when the state of the model is not fully measurable, for physical constraints, or the high cost of sensors, a state observer is added to the command structure.

This soft sensor (observer) is often used for state reconstruction as shown in the figure (see figure 3.4). The state vector variables are estimated using the magnitudes of the inputs and outputs.

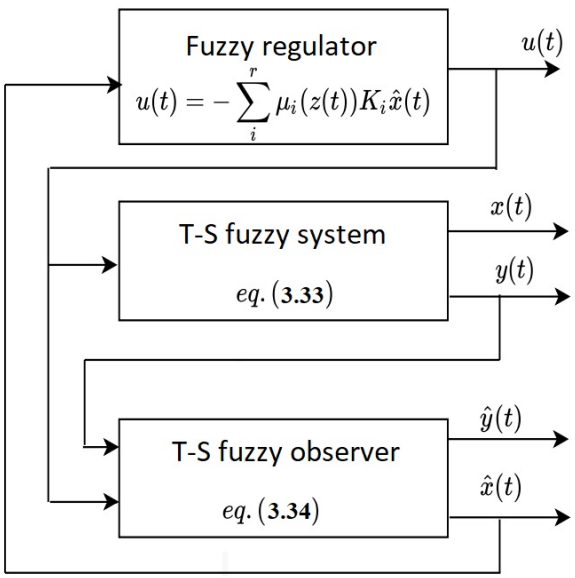

Figure 3.4: Observer-based state reconstruction.

In most work on Takagi-Sugeno fuzzy models, the variables of the premise are assumed to be measurable. However, other models have been developed for synthesis of the observers of these systems, where the variables of the premise are not all measurable [57], [49] [58] [59]. On the other hand, high-gain observers based on the Lyapunov equations, have been treated in the works [60] [61], [62] and [63]. Consider the following Takagi-Sugeno model:

$$\begin{cases} \dot{x}(t) = \sum_{i=1}^{r} \mu_i(z(t)) \left(A_i x(t) + B_i u(t)\right) \\ y(t) = \sum_{i=1}^{r} \mu_i(z(t)) C x(t) \end{cases} \tag{3.33}$$

In the case of a continuous Takagi-Sugeno model, the associated observer is inspired by the one constructed for the linear case. For this, the fuzzy inference of the observer [49] is written as follows:

$$\begin{cases} \dot{\hat{x}}(t) = \sum_{i=1}^{r} \mu_i(\hat{z}(t)) \left(A_i \hat{x}(t) + B_i u(t) + L_i(y(t) - \hat{y}(t))\right) \quad i = 1, \ldots, r \\ \hat{y}(t) = \sum_{i=1}^{r} \mu_i(\hat{z}(t)) C_i \hat{x}(t) \end{cases} \quad i \tag{3.34}$$

where $\hat{x}(t)$ represents the state vector estimated by the fuzzy observer,

L_i are the observer gains, $\hat{z}(t)$ is the estimated premise variable.

The membership function $\mu_i(\hat{z}(t))$ indicates the membership degree of the i^th model associated local, verifying the property of the following convex sum:

$$\begin{cases} \sum_{i=1}^{r} \mu_i(\hat{z}(t)) = 1 \\ 0 \leq \mu_i(\hat{z}(t)) \leq 1 \end{cases} \tag{3.35}$$

The membership function depends on the knowledge or not of the variables of the premises. For this, two cases can be considered:

3.4.3 Measurable premise variable

In the case where the premise is a measurable variable, the work on the design of state observers [58], [41], [57] and [64], are based on the same variables decisions of the model than those of the observer. In fact, in this case, it amounts to replace $\mu_i(\hat{z}(t))$ by $\mu_i(z(t))$.

This then results in a new PDC control law, to stabilize the Takagi-Sugeno fuzzy model (3.34) given by the following equation:

$$u(t) = -\sum_{i=1}^{r} \mu_i(z(t)) K_i \hat{x}(t) \tag{3.36}$$

The gains of the observer (3.36), are determined by the study of the stability of the system generating the state estimation error, defined by:

$$\tilde{x}(t) = x(t) - \hat{x}(t) \tag{3.37}$$

The dynamics of the state estimation error is given by: $\dot{\tilde{x}}(t) = \dot{x}(t) - \dot{\hat{x}}(t)$.

By factoring the activation functions during the dynamics of the state estimation error, we obtain:

$$\dot{\tilde{x}}(t) = \sum_{i=1}^{r} \mu_i(z(t)) \sum_{j=1}^{r} \mu_j(z(t)) \left(A_i - L_i C_i\right) \tilde{x}(t) \tag{3.38}$$

By substituting the first equations of equations (3.33), (3.34) and (3.36), in the dynamics of equation (3.37), we obtain the dynamics of the closed loop with the observer given by:

$$\begin{bmatrix} \dot{x}(t) \\ \dot{\tilde{x}}(t) \end{bmatrix} = \sum_{i=1}^{r}\sum_{j=1}^{r} \mu_i(z(t))\mu_j(z(t)) \begin{bmatrix} A_i - B_iK_i & B_iK_i \\ 0 & A_i - L_iC_j \end{bmatrix} \begin{bmatrix} x(t) \\ \tilde{x}(t) \end{bmatrix} \tag{3.39}$$

A simplification of the expressions described above is possible by setting:

$$G_{ija} = \begin{bmatrix} A_i - B_iK_i & B_iK_i \\ 0 & A_i - L_iC_j \end{bmatrix} \text{ and } \tilde{x}_a(t) = \begin{bmatrix} x(t) \\ \tilde{x}(t) \end{bmatrix} \tag{3.40}$$

We then obtain:

$$\dot{\tilde{x}}_a(t) = \sum_{i=1}^{r}\sum_{j=1}^{r} \mu_i(z(t))\mu_j(z(t))G_{ija}\tilde{x}_a(t) \tag{3.41}$$

Consider the continuous system 3.41. The system is asymptotically stable if and only if there is a matrix $P \in R^{2n\times 2n}$ symmetric positive definite and gains K_i , F_i such that: In this case, the separation principle described in Theorem 6, is presented in the works [41] and [65], making it possible to determine separately, the gains of the controller K_i and the gains of the observer F_i.

Theorem 6 If there are two scalar functions $V(x) : R^n \to R$ and $\hat{V}(\hat{x}) : R^n \to R$ and positive real numbers γ_1, γ_2, γ_3, γ_4, $\hat{\gamma}_1$, $\hat{\gamma}_2$, $\hat{\gamma}_3$ and $\hat{\gamma}_4$ such that .

1.
$$\gamma_1\|x\|^2 \leq V(x) \leq \gamma_2\|x\|^2, \tilde{\gamma}_1\|\tilde{x}\|^2 \leq V(\tilde{x}) \leq \tilde{\gamma}_2\|\tilde{x}\|^2$$

2.
$$\frac{\partial V(x)}{\partial x}\sum_{i=1}^{r}\sum_{j=1}^{r} h_i(z(t))h_j(z(t))\left(A_i - B_iK_j\right)x \leq -\gamma_3\|x\|^2$$
$$\frac{\partial V(\tilde{x})}{\partial \tilde{x}}\sum_{i=1}^{r}\sum_{j=1}^{r} h_i(z(t))h_j(z(t))\left(A_i - L_iC_j\right)\tilde{x} \leq -\tilde{\gamma}_3\|\tilde{x}\|^2$$

3.
$$\left\|\frac{\partial V(x)}{\partial x}\right\|^2 \leq \gamma_4\|x\|^2, \left\|\frac{\partial \tilde{V}(\tilde{x})}{\partial \tilde{x}}\right\|^2 \leq \tilde{\gamma}_4\|\tilde{x}\|^2$$

Then, the complete model 3.41 is globally uniformly asymptotically stable.

Remark. By choosing $V(x) = x^TP_1x$ and $\hat{V}(\hat{x}) = \hat{x}^TP_2\hat{x}$, such that $\hat{V}(\hat{x})$ verifies the control law stability conditions, and observer stability conditions, where conditions (1), (2), and (3) of Theorem 3.7 are satisfied. According to this theorem, the fuzzy controller and observer can be constructed for be independently stable. Thus, if there exist P_1 and P_2 symmetric matrices defined positive of $R_{n\times n}$ and gains K_i and L_i satisfying conditions 3.42, with the following changes of bijective variables: $M_{1i} = K_iP_1$ and $N_{2i} = L_iP_2$

$$\begin{cases} P_1A_i^T - M_i^TB_i^T + A_iP_1 - B_iM_i < 0, i = 1, \ldots, r \\ A_i^TP_2 - C_i^TN_i^T + P_2A_i - N_iC_i < 0, i = 1, \ldots, r \\ P_1A_i^T - M_j^TB_i^T + A_iP_1 - B_iM_j + P_1A_j^T - M_i^TB_j^T + A_jP_1 - B_jM_i < 0, i < j \leq r \\ A_i^TP_2 - C_j^TN_i^T + P_2A_i - N_iC_j + A_i^TP_2 - C_i^TN_j^T + P_2A_j - N_jC_i < 0, i < j \leq r \end{cases} \tag{3.42}$$

3.4.4 Unmeasurable premise variable

The Takagi-Sugeno controller proposed in the previous section, is based on a feedback outputs with measurable state variables. However, the condition estimate is a very wide field of research, for the case of non-measurable state variables. In this case, several difficulties have been used in previous works [66] [67] [47]. Among these, we find Luenberger-type observers who use Lipschitz membership functions [68], with stability conditions formulated as LMIs. Nevertheless, the Lipschist constants which appear in large LMIs reduce the application domains of these observers. Other observers are based on the sliding mode [69], which compensates for the unknown terms of the model.

Yoneyama [70] proposes to consider the variable of the non-measurable premise, as unknown signal where the H_∞ command is used for stability. The premise will be estimated and considered in the calculation of observer rule weights. In [71], the authors assume that the premise variables, depend on the variables estimated by a Takagi-Sugeno fuzzy observer. Therefore, the membership functions of the command are different from those of the Takagi-Sugeno model, because they depend on estimated state variables.

The augmented system based on the Takagi-Sugeno observer (3.34) and the PDC control law given by (3.36), with μ(z(t) = μ(ˆ(t), then becomes:

$$\dot{\bar{x}}(t) = \sum_{i=1}^{r}\sum_{j=1}^{r}\sum_{k=1}^{r} \mu_i(\hat{z}(t))\mu_j(\hat{z}(t))\mu_k(\hat{z}(t))\bar{G}_{ijk}\bar{x}(t) \tag{3.43}$$

$$\bar{x}(t) = \begin{bmatrix} \hat{x}(t) \\ \tilde{x}(t) \end{bmatrix} \tag{3.44}$$

with: $\bar{G}_{ijk} = \begin{bmatrix} A_i - B_iK_k & B_iK_k \\ S^1_{ijk} & S^2_{ijk} \end{bmatrix}$

$$S^1_{ijk} = (A_i - A_j) + (B_i - B_j)K_k - L_j(C_k - C_i)$$

$$S^2_{ijk} = (A_j - L_jC_k) + (B_i - B_j)K_k$$

Theorem 7 The augmented system described by (3.47) is globally asymptotically stable [72], if and only if there exists a common matrix $P > 0$ such that

$$\bar{G}^T_{ijj}P + P\bar{G}_{ijj} < 0 \tag{3.45}$$

$$\left(\frac{\bar{G}_{ijk} + \bar{G}_{ikj}}{2}\right)^T P + P\left(\frac{\bar{G}_{ijk} + \bar{G}_{ikj}}{2}\right) < 0 \tag{3.46}$$

$$\forall i, j < k \in 1, \ldots, n \text{ et } h_i(\hat{z})h_j(\hat{z})h_k(\hat{z}) \neq 0.$$

In this case, the separation principle given by Theorem 6 and the relaxed conditions cannot be used since $\mu(z(t)) \neq \mu(\hat{z}(t))$. Additionally, the constraints employed in this theorem, are not convex, which makes the transformation under LMIs constraints difficult [73].

The principle here then amounts to calculating the gains of the regulator and those of the observer blurred separately and not simultaneously [74].

In this case, we choose the matrix P of the following form:

$$P = \begin{bmatrix} P_1 & 0 \\ 0 & P_2 \end{bmatrix} \tag{3.47}$$

By substituting (3.47) in the conditions given by theorem 7, we will have respectively:

$$\begin{bmatrix} (A_i - B_i K_j)^T P_1 + P_1 (A_i - B_i K_j) & P_1 B_i K_j + S_{ijj}^T P_2 \\ P2 S_{ijj} + K_j B_i^T P1 & E_{ijj} \end{bmatrix} < 0 \tag{3.48}$$

$$\begin{bmatrix} (2A_i - B_i K_k - B_i K_j)^T P_1 + P_1 (2A_i - B_i K_k - B_i K_j) & (*)^T \\ P_2 (S_{ijk} + S_{ikj}) + (K_k + K_j)^T B_i^T P_1 & E_{ijk} + E_{ikj} \end{bmatrix} < 0, j < s \tag{3.49}$$

with $(*)^T$ représente $\left(P_2 (S_{ijk} + S_{ikj}) + (K_k + K_j)^T B_i^T P_1\right)^T$

$$E_{ijk} = ((A_i - L_i C_k) + (B_i - B_j) K_k)^T P_2 + P_2 ((A_i - L_i C_k) + (B_i - B_j) K_k)$$

The LMIs 3.48 and 3.49 are BMIs (Bilinear Matrix inequalities) in P_1, P_2, L_i and K_i which are difficult to solve simultaneously. However, the LMIs given by the following conditions are verified.

$$G_{ij}^T P_1 + P_1 G_{ij} < 0, i, j = 1, \ldots, r \tag{3.50}$$

$$(G_{ik} + G_{ij})^T P_1 + P_1 (G_{ik} + G_{ij}) < 0, j < s \tag{3.51}$$

with: $G_{ik} = A_i - B_i K_k$, whose linearization is easy to obtain by the methods classical change of variables.

Thus, the matrices P_1 and K_i are then replaced in equations 3.48 and 3.49, by their respective values P_1^{opt} and K_i^{opt} .

In this case, the LMIs system obtained also becomes linear in P_2 and Y_i with $Y_i = P_2 L_i$. .

3.4.5 DFIG Takagi-Sugeno Fuzzy Model

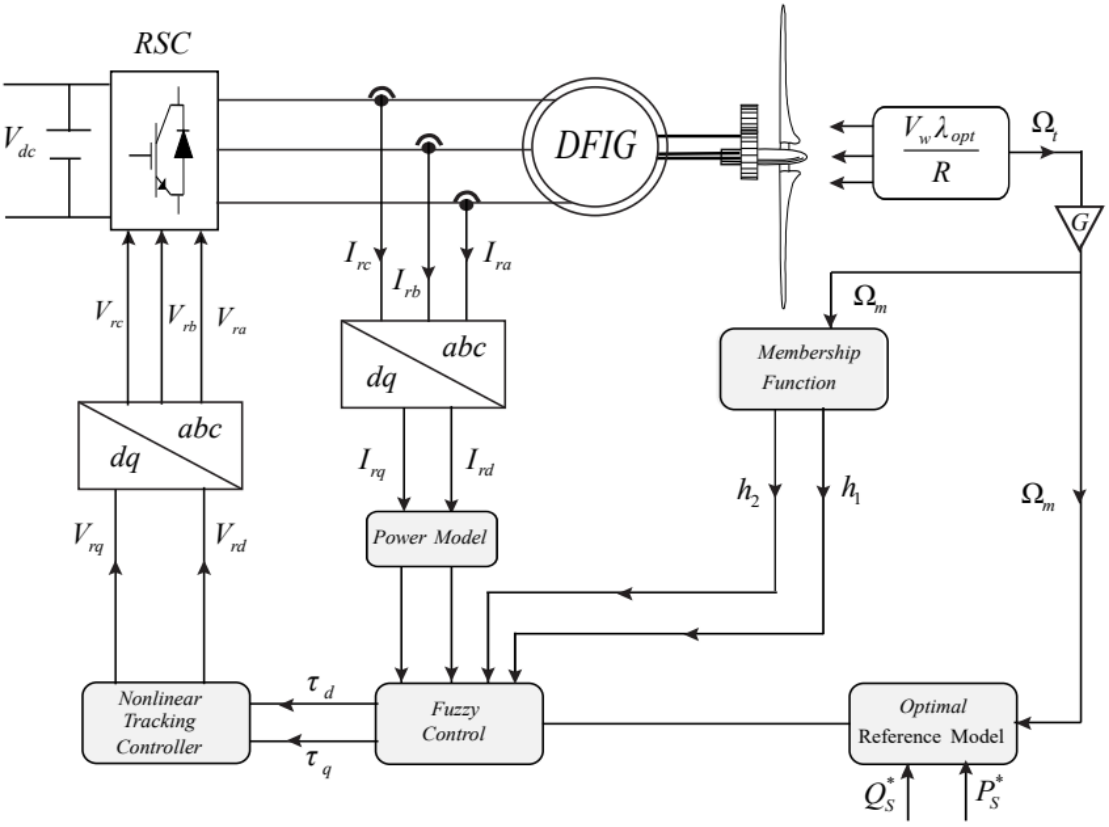

Figure 3.5: WECS based on DFI-Generator with the control strategy proposed.

The state space of the Double Feed Induction Generator dynamics model is expressed by the following equations 3.62

$$\begin{cases} \dot{x}(t) = Ax(t) + Bu(t) \\ y(t) = Cx(t) \end{cases} \tag{3.52}$$

with

$$\begin{cases} x(t) = \begin{bmatrix} I_{rd} & I_{rq} \end{bmatrix}^T \\ u(t) = \begin{bmatrix} V_{rd} & V_{rq} \end{bmatrix}^T \\ y(t) = \begin{bmatrix} P_s & Q_s \end{bmatrix}^T \end{cases} \tag{3.53}$$

and

$$A = \begin{bmatrix} -\mathrm{R_r}/\left(\mathrm{L_r}\sigma\right) & \mathrm{gw_s} \\ -\mathrm{gw_s} & -\mathrm{R_r}/\left(\mathrm{L_r}\sigma\right) \end{bmatrix} \tag{3.54}$$

$$B = \begin{bmatrix} 1/\left(\mathrm{L_r}\sigma\right) & 0 \\ 0 & 1/\left(\mathrm{L_r}\sigma\right) \end{bmatrix} \tag{3.55}$$

$$C = \begin{bmatrix} 0 \\ -\mathrm{gV_sL_m/L_s} \end{bmatrix} \tag{3.56}$$

Where the leakage coefficient σ is given by:

$$\sigma = 1 - \frac{L_m^2}{L_r L_s} \tag{3.57}$$

The sector of nonlinearities of $\Omega_s(t)$ is bounded

$$\underline{\Omega}_s \leq \Omega_s(t) \leq \overline{\Omega}_s \tag{3.58}$$

Thus, the premise variable then becomes:

$$\Omega_s(t) = F_1\overline{\Omega}_s(t) + F_2\underline{\Omega}_s \tag{3.59}$$

where F1, F2 denote the grade of membership functions that can be defined as follows:

$$F_1 = \frac{\Omega_s(t) - \underline{\Omega}_s}{\overline{\Omega}_s - \underline{\Omega}_s} \quad F_2 = \frac{\overline{\Omega}_s - \Omega_s(t)}{\overline{\Omega}_s - \underline{\Omega}_s} \tag{3.60}$$

The fuzzy model for a dynamic system is descibed by a finite set of fuzzy IF ... THEN rules as follow:

rule 1: if $\Omega_s(t)$ is F1 then

$$\begin{cases} \dot{x}(t) = A_1x(t) + B_1u(t) \\ y(t) = C_1x(t) \end{cases} \tag{3.61}$$

rule 2: if $\Omega_s(t)$ is F2 then

$$\begin{cases} \dot{x}(t) = A_2x(t) + B_2u(t) \\ y(t) = C_2x(t) \end{cases} \tag{3.62}$$

Where:

$$A_1 = \begin{bmatrix} -R_r/(L_r\sigma) & g\overline{\Omega_s} \\ g\overline{\Omega_s} & -R_r/(L_r\sigma) \end{bmatrix} \tag{3.63}$$

$$A_2 = \begin{bmatrix} -R_r/(L_r\sigma) & g\underline{\Omega_s} \\ g\underline{\Omega_s} & -R_r/(L_r\sigma) \end{bmatrix} \tag{3.64}$$

$$B_1 = B_2 = \begin{bmatrix} 1/(L_r\sigma) & 0 \\ 0 & 1/(L_r\sigma) \end{bmatrix} \tag{3.65}$$

$$C_1 = C_2 = \begin{bmatrix} 0 \\ -gV_sL_m/L_s \end{bmatrix} \tag{3.66}$$

The global fuzzy model is inferred as follows:

$$\dot{x}(t) = \sum_{i=1}^{2} h_i(\Omega_s(t))\{A_ix(t) + B_iu(t)\} \tag{3.67}$$

Where

$$h_i(\Omega_s(t)) = \frac{F_i(\Omega_s(t))}{\sum_{i=1}^{2} F_i(\Omega_s(t))} \tag{3.68}$$

It is obvious that $\sum_{i=1}^{2} h_i(\Omega_s(t)) = 1$ with $h_i(\Omega_s(t)) \geq 0$

3.4.6 Tracking DFIG Control of Active And Reactive Power

TS Fuzzy Controller based Power Control

Most of the existing research deals with the efficiency of the T-S model system.
However, these only make it possible to guarantee the return of the non-linear system to a point of equilibrium starting from non-zero initial conditions.
Let

$$\tilde{x}(t) = x(t) - x_{op}(t) \tag{3.69}$$

be defined as the tracking error and its time derivative is given by:

$$\dot{\tilde{X}}(t) = \dot{x}(t) - \dot{x}_{op}(t) \tag{3.70}$$

The purpose is to drive the state variable to follow the optimal reference such that

$$x(t) - x_{op}(t) \longrightarrow 0, t \longrightarrow \infty \tag{3.71}$$

by replacing the term of Eq. 3.72 into Eq.3.70, this later becomes

$$\dot{x}(t) = \sum_{i=1}^{2} h_i(\Omega_s(t))\{A_i\tilde{x}(t) + B_i u(t) + A_i x_{op}(t) - \dot{x}_{op}(t)\} \tag{3.72}$$

ntroducing the new control variable $\tau(t)$that satisfy the following relation:

$$\sum_{i=1}^{2} h_i(\Omega_s(t))B_i\tau(t) = \sum_{i=1}^{2} h_i(\Omega_s(t))\{B_i u(t) + A_x op(t)\} - \dot{x}_{op}(t) \tag{3.73}$$

The TS controllers is performed through the parallel distributed compensation technique
Controller rule i = 1, 2

$$\dot{x}(t) = \sum_{i=1}^{2} h_i(\Omega_s(t))\{A_i\tilde{x}(t) + B_i\tau(t)\} \tag{3.74}$$

The overall PDC controller is inferred as follows

$$\tau(t) = -\sum_{j=1}^{2} h_j(\Omega_s(t))K_j\tilde{x}(t) \tag{3.75}$$

Combining eq.3.76 with eq.3.74, the closed-loop fuzzy system is written as

$$\dot{\tilde{X}}(t) = \sum_{i=1}^{2}\sum_{j=1}^{2} h_i(\Omega_s(t))h_j(\Omega_s(t))G_{ij}\tilde{x}(t) \tag{3.76}$$

Where:

$$G_{ij} = A_i - B_i K_j \tag{3.77}$$

In order to determine the conditions stability of the TS fuzzy system, the Lyapunov approach is considered.

The Takagi-Sugeno fuzzy system (28) is stable if the following LMIs hold are satisfied :

for i = j

$$QA_i^T + A_iQ - M_i^T B_i^T - B_iM_i + \alpha Q < 0 \tag{3.78}$$

for i $\neq$ j

$$QA_i^T + A_iQ - M_j^T B_i^T - B_iM_j + \alpha Q < 0 \tag{3.79}$$

Where

$$Q = P^{-1}, K_j = M_jQ^{-1} \tag{3.80}$$

and α positif scalar

Optimal reference controller and nonlinear tracking control

$$\sum_{i=1}^{2} h_i(\Omega_s(t))B_i\tau(t) = \sum_{i=1}^{2} h_i(\Omega_s(t))B_iu(t) + A_ix_{op}(t) - \dot{x_{op}}(t) \tag{3.81}$$

$$A = \sum_{i=1}^{2} h_iA_i, B = \sum_{i=1}^{2} h_iB_i \tag{3.82}$$

$$B((u(t)) - \tau(t)) = A(\Omega_s)x_{op}(t) - \dot{x_{op}}(t) \tag{3.83}$$

$$\begin{bmatrix} \frac{1}{L_r\sigma} & 0 \\ 0 & \frac{1}{L_r\sigma} \end{bmatrix} \begin{bmatrix} V_d - \tau_d \\ V_q - \tau_q \end{bmatrix} = \begin{bmatrix} \frac{-R_r}{L_r\tau} & gw_s \\ -gw_s & -\frac{R_r}{L-r\sigma} \end{bmatrix} \begin{bmatrix} I_{drop} \\ I_{qrop} \end{bmatrix} - \frac{d}{dt} \begin{bmatrix} I_{drop} \\ I_{qrop} \end{bmatrix} \tag{3.84}$$

$$\begin{cases} V_{rd} = \tau_d + R_rI_{drop} - gL_r\sigma\Omega_sIqrop + L_r\sigma Iqrop \\ V_{rq} = \tau_q + gL_r\sigma\Omega_sIdrop + R_rI_{qrop} + \frac{gV_sL_m}{\sigma L_rL_s} + L_r\sigma Iqrop \end{cases} \tag{3.85}$$

3.5 Simulation

We evaluated this control strategy through the application on $Matlab$ and $Simulink$ and we obtained following the results:

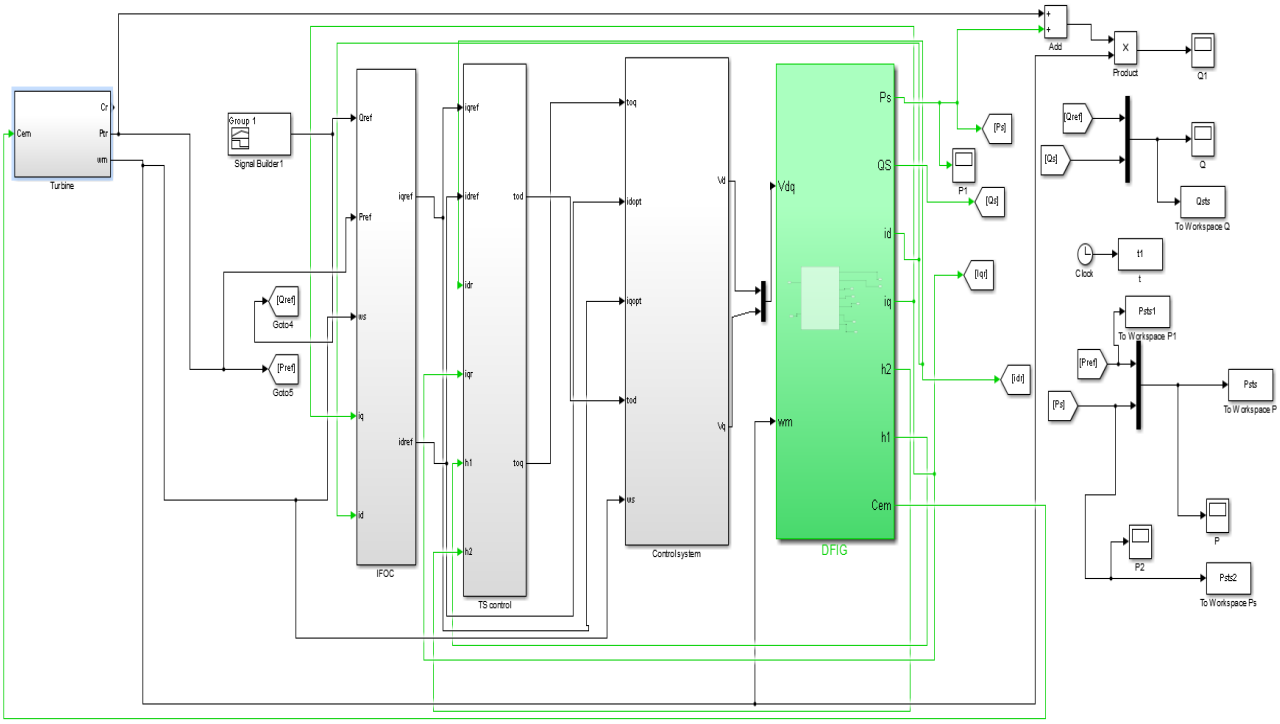

Figure 3.6: General diagram.

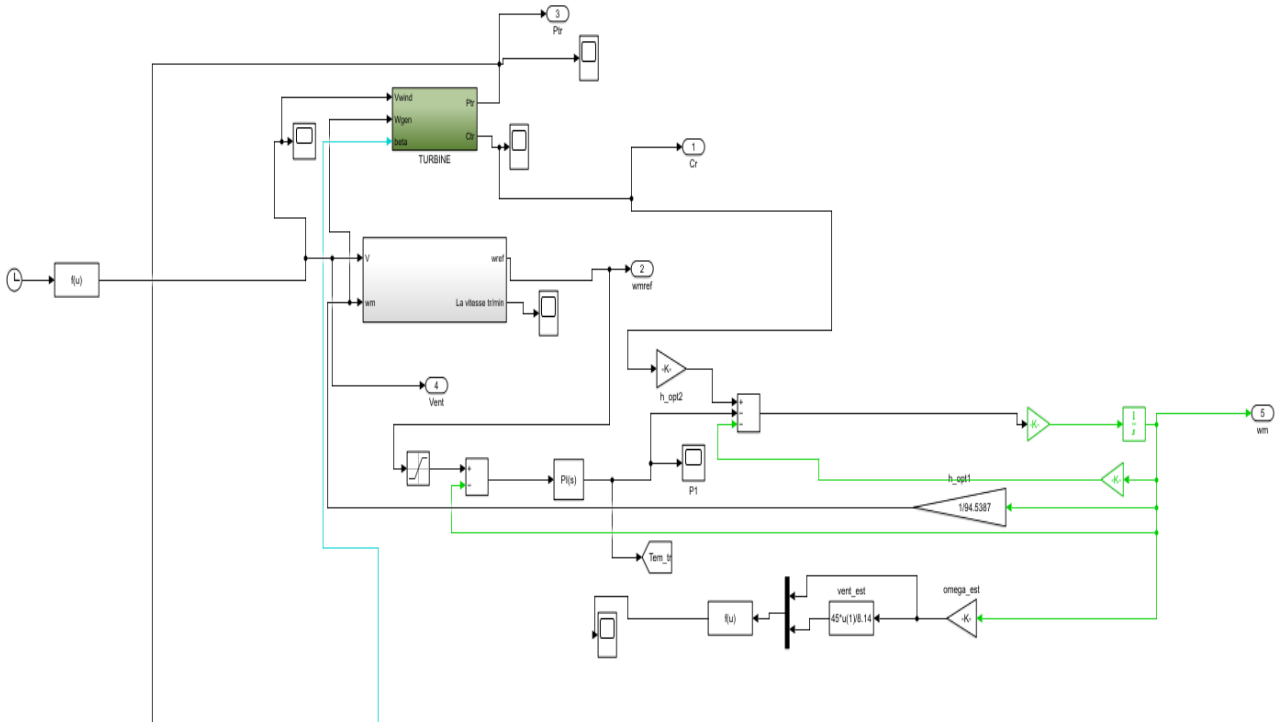

Figure 3.7: The wind turbine diagram.

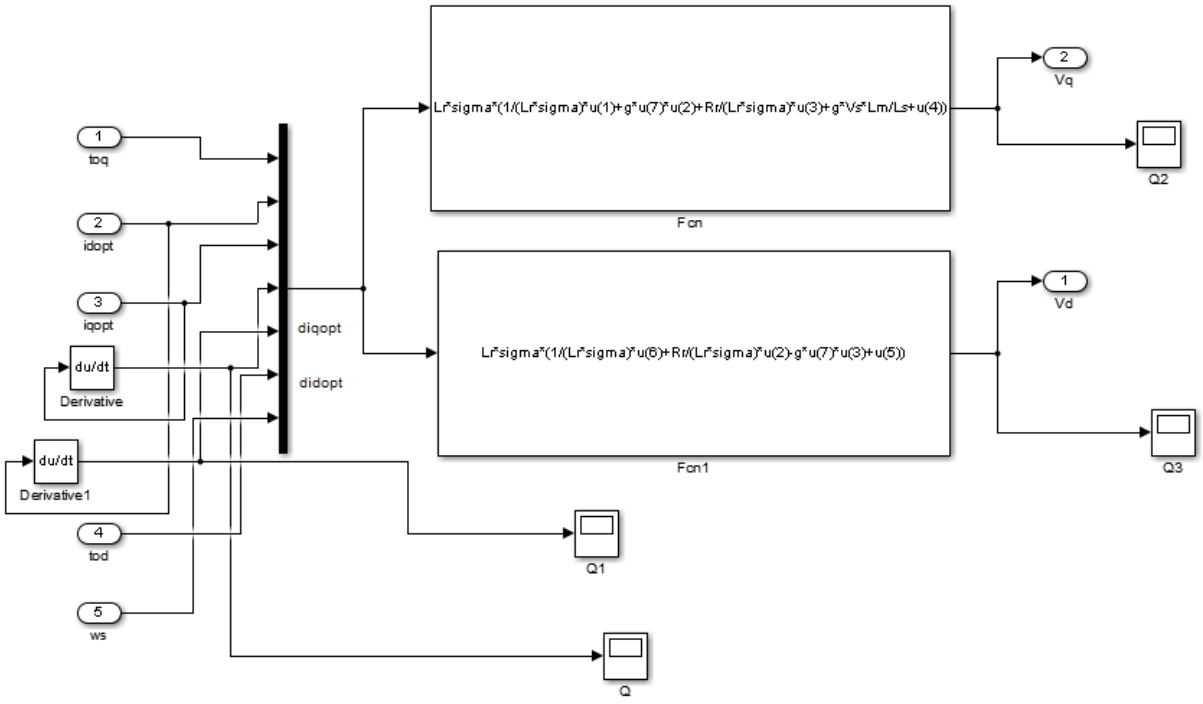

Figure 3.8: T-S controller diagram design.

We have tested our controller with the following signal as wind profile to see if he'd follow

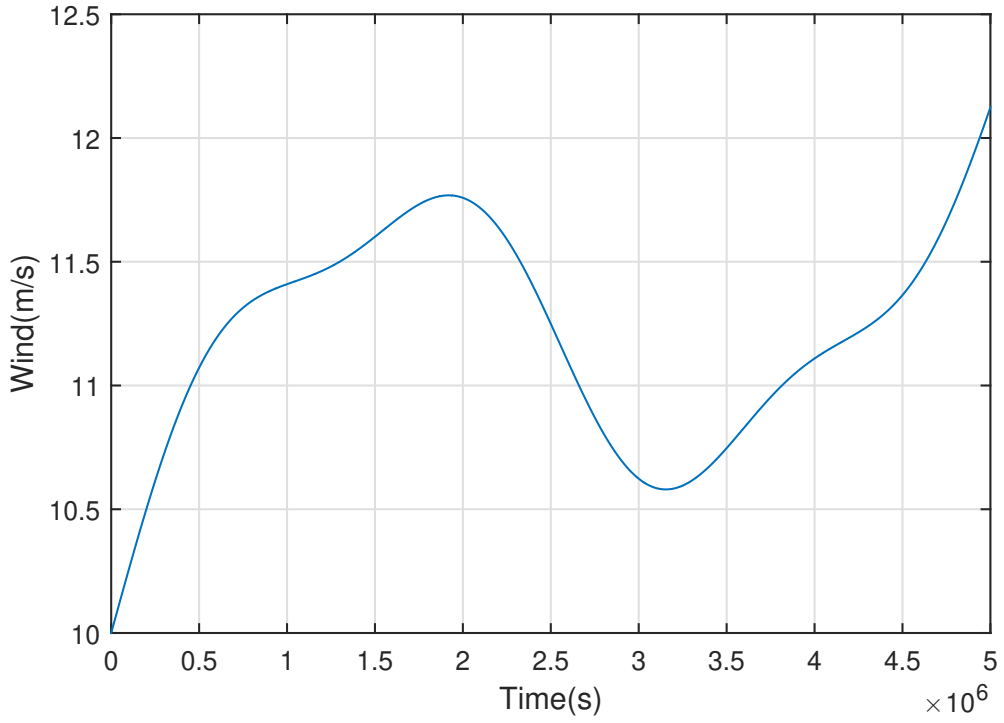

Figure 3.9: Real Wind speed profile. V_{wind}.

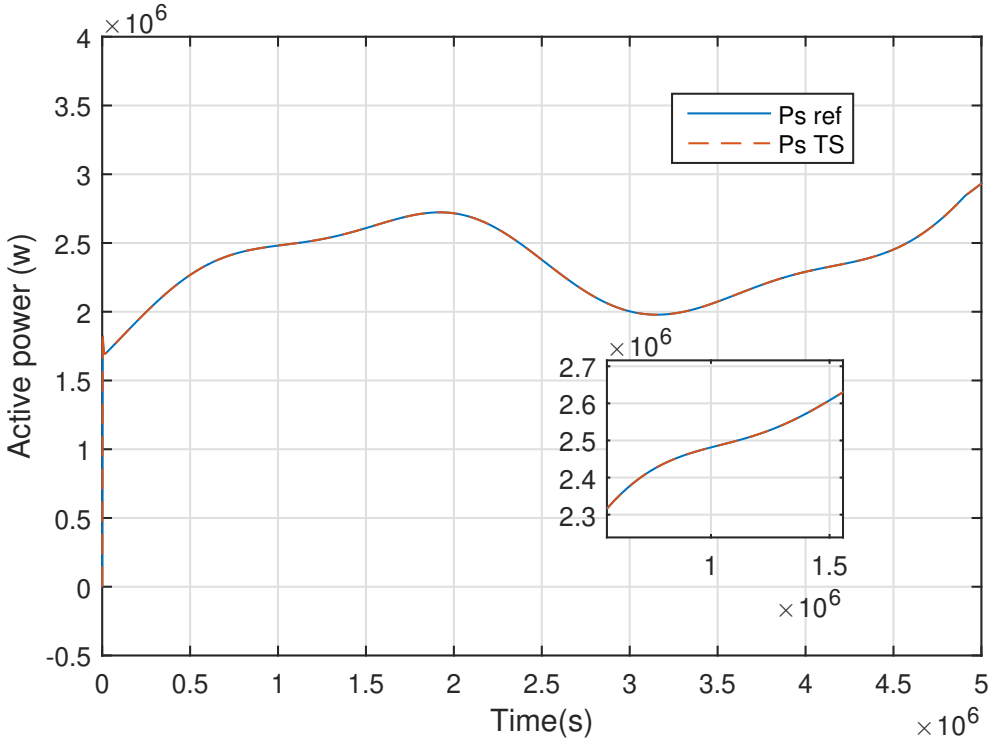

Figure 3.10: Response of the active power of real wind profile P_s.

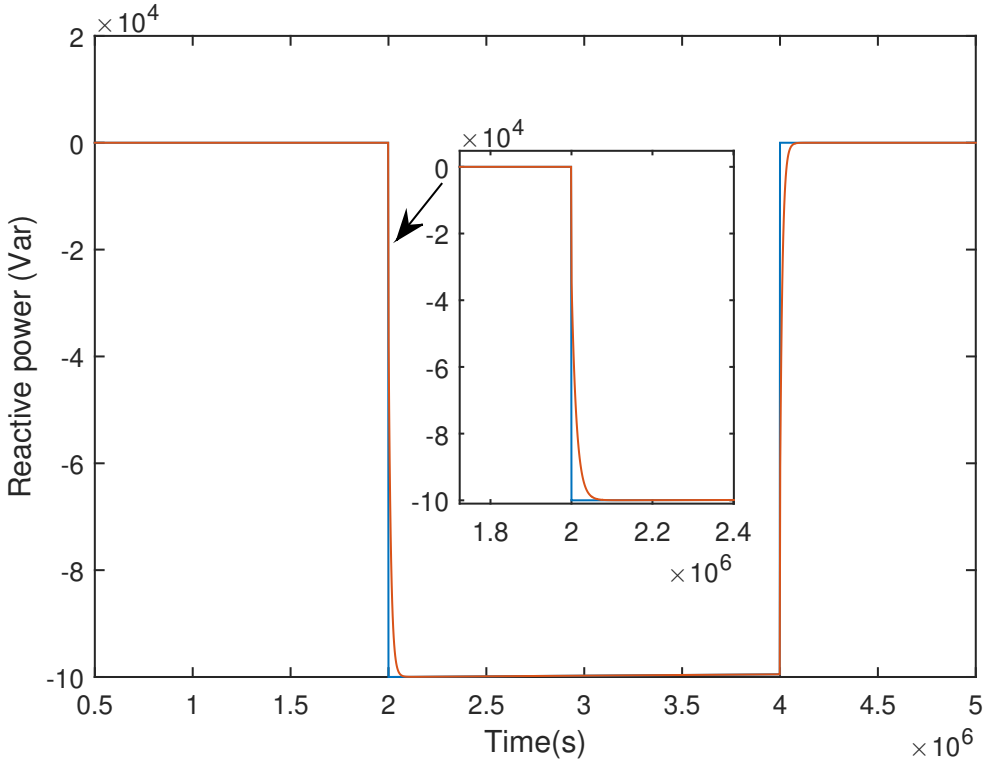

Figure 3.11: Response of the reactive power of real wind profile Q_s.

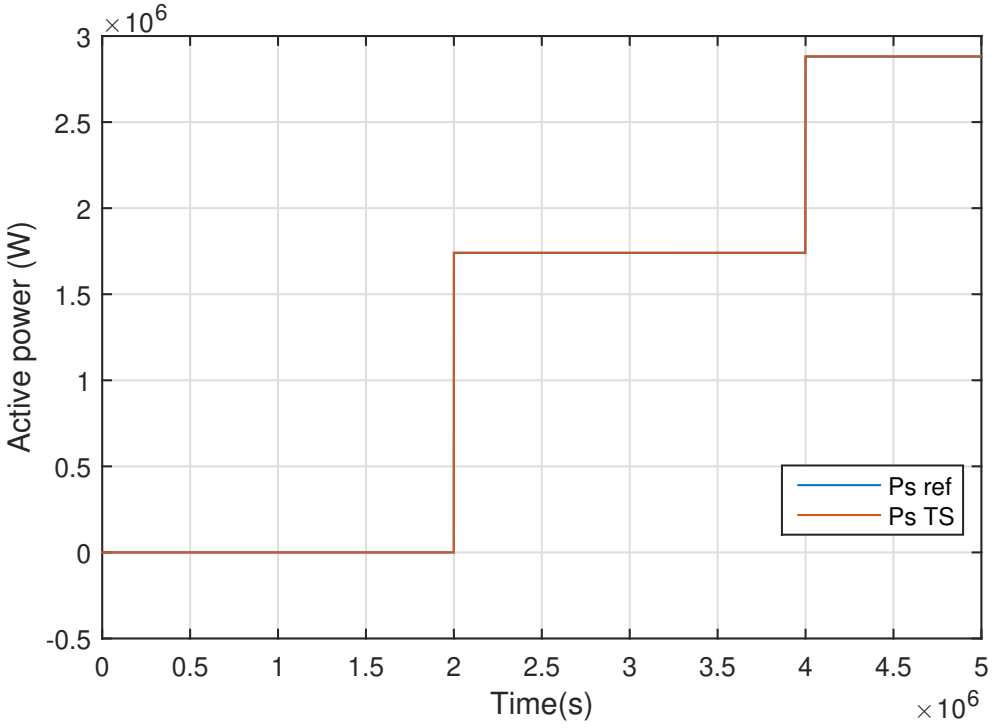

Figure 3.12: Response of the active power of fixed signal P_s.

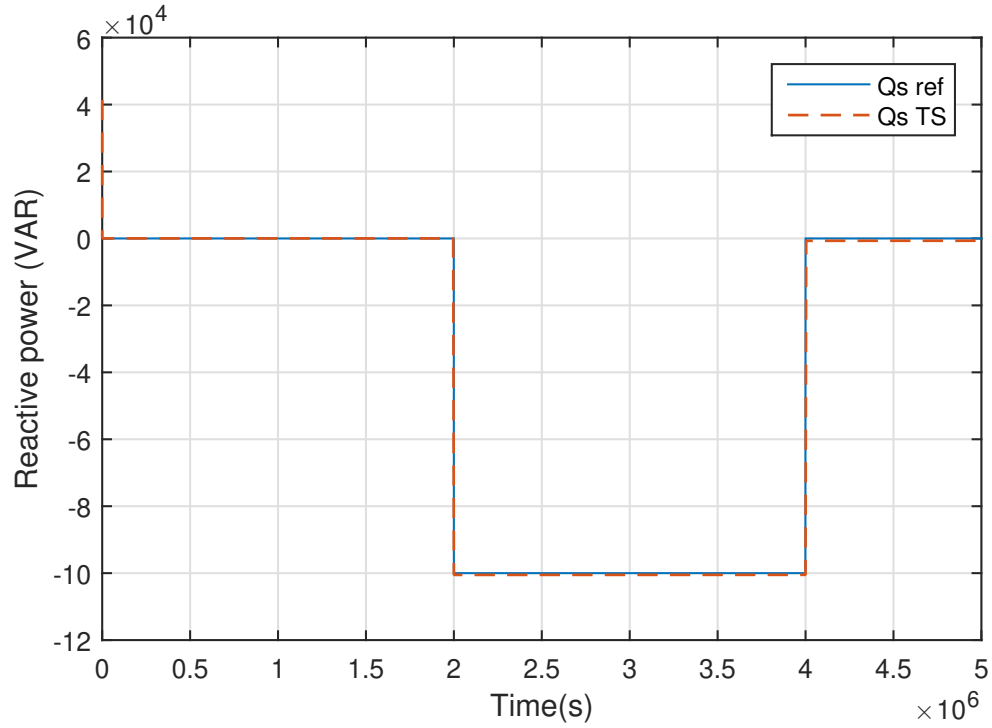

Figure 3.13: Response of the reactive power of fixed signal Q_s.

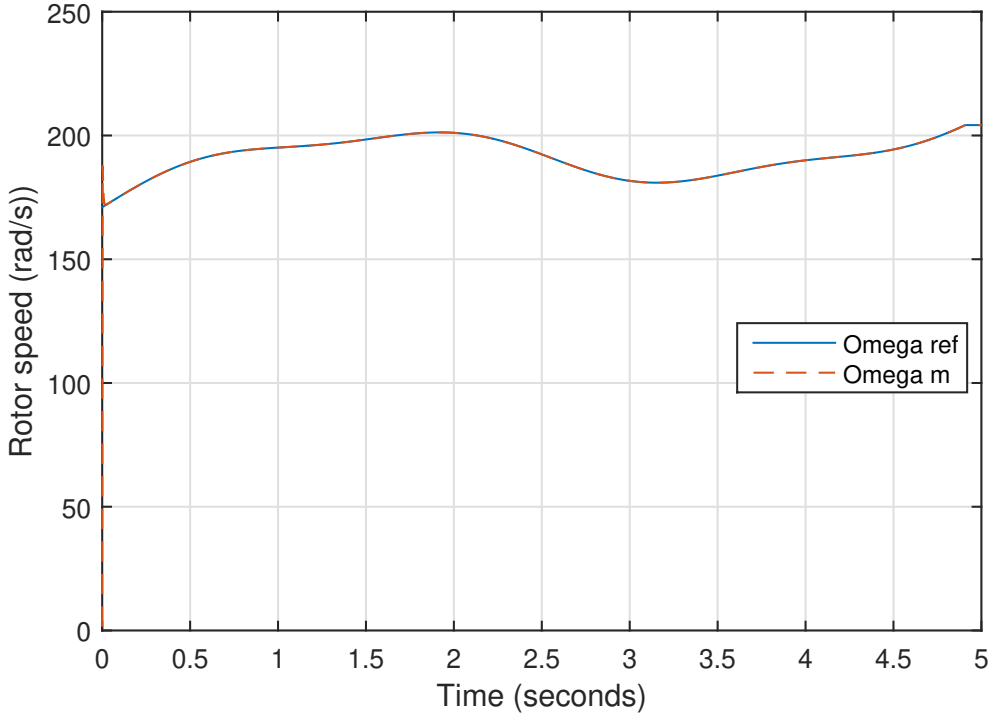

Figure 3.14: Response of the rotor speed .

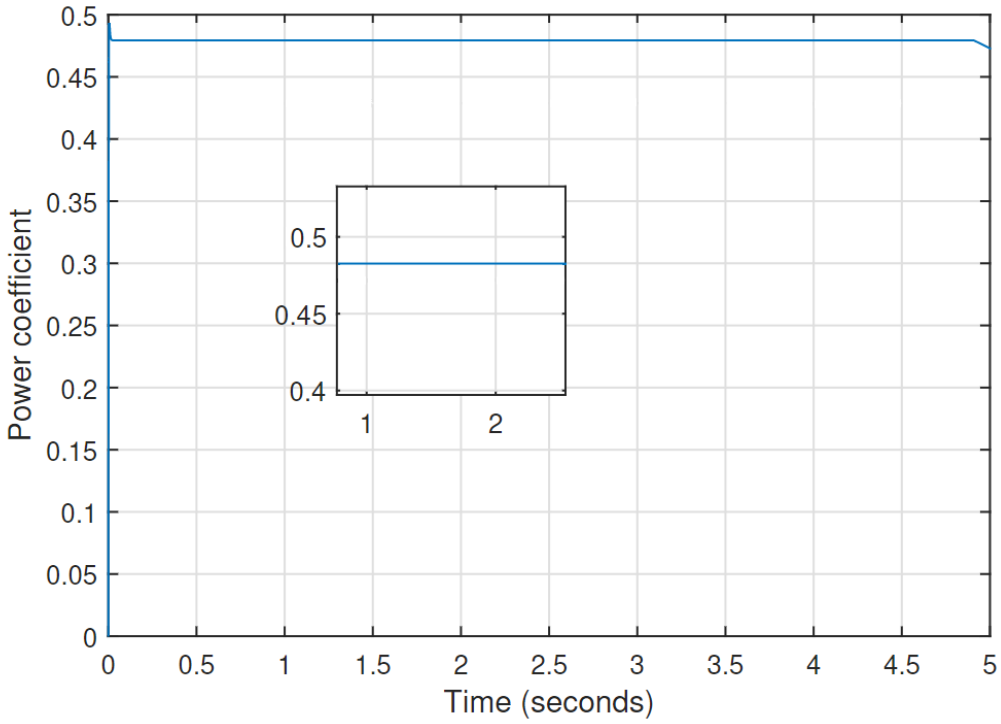

Figure 3.15: Power Coefficient C_p.

3.6 Conclusion

In this chapter, we have introduced the structure of fuzzy models Takagi-Sugeno and for the stabilization of this model, we used a PDC control law, which is based on the Lyapunov function to ensure the convergence of the closed-loop fuzzy model. And for the stability of the Takagi-Sugeno fuzzy system, we confirmed the LMIs conditions are satisfied.

And with obtained results through the simulation in MATLAB / Simulink, we confirmed that our controller is working.

Conclusion

The most famous Takagi Sugano fuzzy controller model was Developed and applied to a variable speed wind energy conversion system based on DFI-generator. firstly, The focus of this work is to control wind turbines by design MPPT technology. So this extracts the maximum available power Rotor speed control.

Secondly, introduces the control of the machine-side converter. This is dedicated to active and reactive power control of DFI-generators. It can be controlled by acting on the rotor current. Here the Takagi-Sugeno fuzzy model is designed as the controller. To demonstrate the effectiveness and system stability of the proposed controller, a comparison with a PI controller under sudden wind speed changes is performed using Matlab Simulink. In fact, the simulation results show that the controlled DFIG system using the Takagi-Sugeno fuzzy control model is characterized by a robust response independent of mutation. Furthermore, the controller guarantees excellent performance in terms of stability, tracking and robustness against disturbances, faster response time and less overshoot compared to the classic PI controller.

References

[1] Kevin E Trenberth. *Climate change caused by human activities is happening and it already has major consequences*. 2018.

[2] Venkata Yaramasu et al. *PMSG-based wind energy conversion systems: survey on power converters and controls*. 2017.

[3] Yun Wang et al. *Approaches to wind power curve modeling: A review and discussion*. 2019.

[4] Lucy Y Pao and Kathryn E Johnson. *A tutorial on the dynamics and control of wind turbines and wind farms*. IEEE, 2009.

[5] Mukhtiar Singh. *Adaptive network-based fuzzy inference systems for sensorless control of PMSG based wind turbine with power quality improvement features*. 2010.

[6] Iman Poultangari, Reza Shahnazi, and Mansour Sheikhan. *RBF neural network based PI pitch controller for a class of 5-MW wind turbines using particle swarm optimization algorithm*. 2012.

[7] Kuo-Ho Su, Chung-Chun Kung, and Ti-Hung Chen. *Design and applications of strategy-oriented hybrid intelligent controller for nonlinear dynamical system*. IEEE, 2007.

[8] Badr Mansouri et al. *Output feedback LMI tracking control conditions with H∞ criterion for uncertain and disturbed T–S models*. 2009.

[9] Farid Boumaraf. *Commande intelligente d'une association convertisseur statique machine asynchrone à double alimentation*. 2009.

[10] GWEC – Global Wind Energy Council. *global wind report 2022*. URL: https://www.gwec.net.

[11] Thomas Ackermann and Lennart Söder. *Wind energy technology and current status: a review*. 2000.

[12] D. Wood. *Small wind turbines analysis, design, and application. New York*. 2011.

[13] Mohammed Guezgouz et al. *Assessment of solar and wind energy complementarity in Algeria*. 2021.

[14] Zhour Abada and Malek Bouharkat. *Study of management strategy of energy resources in Algeria*. 2018.

[15] Algerian Ministry of Energy. *The New National Renewable Energy Development Program 2015-2030*. URL: https://www.energy.gov.dz/.

[16] O. Bennouna. *diagnostic des systèmes linéaires dynamiques application à un système à énergie renouvelable de type éolien*. 2006.

[17] F. Poitiers. *Etude et Commande de Génératrices Asynchrones pour l'Utilisation de L'Energie Eolienne*. 2003.

[18] Vladislav Akhmatov. *Full-load converter connected asynchronous generators for MW class wind turbines*. 2005.

[19] Frede Blaabjerg and Zhe Chen. *Power electronics for modern wind turbines*. 2005.

[20] Venkata Yaramasu et al. *High-power wind energy conversion systems: State-of-the-art and emerging technologies*. 2015.

[21] Sousso Kelouwani and Kodjo Agbossou. *Nonlinear model identification of wind turbine with a neural network*. 2004.

[22] G.Elliot R.Hunter. *Wind-Diesel Systems : A guide to the technology and its implementation*. 1994.

[23] Shwe Hlaing. *Basic concepts of doubly fed induction generator driven by wind energy conversion system*. 2014.

[24] H.Hansen. *Conceptual Survey of Generators and Power Electronics for Wind Turbines*. 2001.

[25] Tomonobu Senjyu et al. *Operation strategies for stability of gearless wind power generation systems*. IEEE, 2008.

[26] H Bensaid. *The Algerian programme on wind energy*. 1985.

[27] Víctor Hugo Grisales Palacio et al. *Takagi-Sugeno fuzzy modeling and control applied ̀to a wastewater treatment bioprocess 'ees*. 2007.

[28] Youcef Elbia. *Optimized fuzzy control of an asynchronous machine à double feed and à flux orientedè*. 2009.

[29] Ihssen Hamzaoui. *Modélization of the asynchronous machine ẁith double supply for its use as aérogénérator*. 2008.

[30] *Study and control of a wind power system à based on a double powered electric machine, author=Khettache, Ugly, year=2007, school=Batna, Université El Hadj Lakhdar. Faculty of Engineering Sciences*.

[31] *Control-command of an asynchronous generator ̀dual-powered with storage system for production ẁind turbine, author=Boyette, Armand, year=2006, school=Université Henri Poincaré-Nancy 1*.

[32] Lei Sun et al. *Active power and reactive power regulation capacity study of DFIG wind turbine*. IEEE, 2009.

[33] T Ghennam, EM Berkouk, and B Francois. *Modeling and control of a doubly fed induction generator (DFIG) based wind conversion system*. IEEE, 2009.

[34] Nicolas Patin, Eric Monmasson, and Jean-Paul Louis. *Modeling and control of a cascaded doubly fed induction generator dedicated to isolated grids*. 2009.

[35] Shiyi Shao et al. *Stator-flux-oriented vector control for brushless doubly fed induction generator*. 2009.

[36] Xueqin Zheng and Donghui Guo. *Study on the Connection of DFIG to Grid Based on Double-vector PWM*. IEEE, 2010.

[37] Abdelkader Akhenak. *Design of nonlinear observers by multimodel approach: application to diagnosis*. 2004.

[38] Hua O Wang and Kazuo Tanaka. *Fuzzy control systems design and analysis: A linear matrix inequality approach*. 2004.

[39] Tomohiro Takagi and Michio Sugeno. *Fuzzy identification of systems and its applications to modeling and control*. 1985.

[40] Komi Gasso. *Identification of non-linear dynamical systems: multi-model approach*. 2000.

[41] Xiao-Jun Ma, Zeng-Qi Sun, and Yan-Yan He. *Analysis and design of fuzzy controller and fuzzy observer*. 1998.

[42] Mohamed Yacine HAMMOUDI. *Contribution à la commande et à l'observation dans l'association convertisseurs machine*. 2015.

[43] Tahar Bouarar. *Contribution ̀to the synthesis of control laws for uncertain and perturbed Takagi-Sugeno type descriptors*. 2009.

[44] Lotfi Moussaoui et al. *State and output feedback control for constrained discrete-time nonlinear systems*. 2019.

[45] Alexandr Mikhailovich Liapounoff. *Probleme General de la Stabilite du Mouvement.(AM-17), Volume 17*. 2016.

[46] Stephen Boyd et al. *Linear matrix inequalities in system and control theory*. 1994.

[47] Kazuo Tanaka and Michio Sugeno. *Stability analysis and design of fuzzy control systems*. 1992.

[48] Hua O Wang, Kazuo Tanaka, and Michael F Griffin. *An approach to fuzzy control of nonlinear systems: Stability and design issues*. 1996.

[49] Kazuo Tanaka, Takayuki Ikeda, and Hua O Wang. *Fuzzy regulators and fuzzy observers: relaxed stability conditions and LMI-based designs*. 1998.

[50] Prakash Mani et al. *Digital controller design via LMIs for direct-driven surface mounted PMSG-based wind energy conversion system*. 2019.

[51] Naoual Tidjani, Abderrezek Guessoum, and Djamel Ounnas. *Permanent-Magnet Synchronous Generator Wind Turbine based on Takagi-Sugeno Fuzzy Models*. IEEE, 2019.

[52] Euntai Kim and Heejin Lee. *New approaches to relaxed quadratic stability condition of fuzzy control systems*. 2000.

[53] Kazuo Tanaka, Masataka Nishimura, and Hua O Wang. *Multi-objective fuzzy control of high rise/high speed elevators using LMIs*. IEEE, 1998.

[54] L El Ghaoui. *Approche lmi pour la commande: une introduction*. 1997.

[55] P Gahinet et al. *LMI control toolbox-for use with Matlab, Natick, MA: The MATH Works*. 1995.

[56] Sung Kyung Hong and Yoonsu Nam. *Stable fuzzy control system design with pole-placement constraint: an LMI approach*. 2003.

[57] Kazuo Tanaka and Manabu Sano. *A robust stabilization problem of fuzzy control systems and its application to backing up control of a truck-trailer*. 1994.

[58] Gang Feng et al. *Design of fuzzy control systems with guaranteed stability*. 1997.

[59] Sabizhan Sumbekov, Bui Duc Hong Phuc, and Ton Duc Do. *Takagi–Sugeno fuzzy-based integral sliding mode control for wind energy conversion systems with disturbance observer*. 2020.

[60] FE Thau. *Observing the state of non-linear dynamic systems*. 1973.

[61] Murat Arcak and Petar Kokotovic. *Observer-based control of systems with slope-restricted nonlinearities*. 2001.

[62] Jean-Paul Gauthier, Hassan Hammouri, and Sami Othman. *A simple observer for nonlinear systems applications to bioreactors*. 1992.

[63] John Tsinias. *Observer design for nonlinear systems*. 1989.

[64] Kazuo Tanaka, Takayuki Ikeda, and Hua O Wang. *Robust stabilization of a class of uncertain nonlinear systems via fuzzy control: quadratic stabilizability, H/sup/spl infin//control theory, and linear matrix inequalities*. 1996.

[65] Jun Yoneyama et al. *Design of output feedback controllers for Takagi–Sugeno fuzzy systems*. 2001.

[66] Thierry-Marie Guerra et al. *Conditions of output stabilization for nonlinear models in the Takagi–Sugeno's form*. 2006.

[67] K-Y Lian and J-J Liou. *Output tracking control for fuzzy systems via output feedback design*. 2006.

[68] Pontus Bergsten and Rainer Palm. *Thau-Luenberger observers for TS fuzzy systems*. IEEE, 2000.

[69] Pontus Bergsten, Rainer Palm, and Dimiter Driankov. *Observers for Takagi-Sugeno fuzzy systems*. 2002.

[70] Jun Yoneyama. *Output feedback control for fuzzy systems with immeasurable premise variables*. IEEE, 2009.

[71] Mohammed Chadli, Didier Maquin, and Jos Ragot. *Observer-based controller for Takagi-Sugeno models*. IEEE, 2002.

[72] Yann Morere. *Implementation of control laws for fuzzy models of the Takagi-Sugeno type*. 2001.

[73] Dalil Ichalal et al. *Design of Observers for Takagi-Sugeno Systems with Immeasurable Premise Variables: an □2 Approach*. 2008.

[74] Shiyu Yan and Zengqi Sun. *Study on separation principles for T–S fuzzy system with switching controller and switching observer*. 2010.